

This is an author-created, un-copyedited version of an article published in the Journal of Neural Engineering. IOP Publishing Ltd is not responsible for any errors or omissions in this version of the manuscript or any version derived from it. The Version of Record is available online at <https://doi.org/10.1088/1741-2552/adb335>

1
2
3 **Master classes of the tenth international brain-computer interface meeting:**
4 **showcasing the research of BCI trainees**
5

6 Authors: Stephanie Cernera^{1*}, Tan Gemicioglu^{2*}, Julia Berezutskaya³, Richard Csaky⁴,
7 Maxime Verwoert⁵, Daniel Polyakov^{6,7}, Sotirios Papadopoulos^{8,9,10}, Valeria Spagnolo¹¹,
8 Juliana Gonzalez Astudillo¹², Satyam Kumar¹³, Hussein Alawieh¹³, Dion Kelly¹⁴, Joanna
9 R.G. Keough¹⁴, Araz Minhas¹⁴, Matthias Dold¹⁵, Yiyuan Han¹⁶, Alexander
10 McClanahan¹⁷, Mousa Mustafa¹⁸, Juan Jose Gonzalez-Espana¹⁹, Florencia Garro²⁰,
11 Angela Vujic²¹, Kriti Kacker²², Christoph Kapeller²³, Simon Geukes³, Ceci
12 Verbaarschot²⁴, Michael Wimmer²⁵, Mushfika Sultana²⁶, Sara Ahmadi¹⁶, Christian
13 Herff²⁷, Andreea Ioana Sburlea²⁸, Camille Jeunet²⁹, David E. Thompson³⁰, Marianna
14 Semprini³¹, Richard Andersen³², Sergey Stavisky³³, Eli Kinney-Lang³⁴, Fabien Lotte³⁵,
15 Jordy Thielen¹⁶, Xing Chen³⁶, Victoria Peterson¹¹, Aysegul Gunduz³⁷, Theresa
16 Vaughan^{38**}, Davide Valeriani^{39**}
17
18
19

20 Corresponding author:
21

22 Stephanie Cernera
23

24 Email: stephcernera@gmail.com
25

26 *co-first authors
27

28 **co-last authors
29

30 Affiliations
31

32 ¹ Department of Neurological Surgery, University of California San Francisco, San
33 Francisco, CA, USA
34

35 ²School of Information Science, Cornell University, New York, NY, USA
36

37 ³Brain Center, Department of Neurology & Neurosurgery, University Medical Center
38 Utrecht, Utrecht 3584 CX, Netherlands
39

40 ⁴ Department of Psychiatry, University of Oxford
41

42 ⁵ Department of Neurosurgery, Mental Health and Neuroscience Research Institute,
43 Maastricht University, Maastricht, The Netherlands
44

45 ⁶ Department of Cognitive and Brain Sciences, Ben-Gurion University of the Negev,
46 Be'er Sheva, Israel
47

48 ⁷ Agricultural, Biological, Cognitive Robotics Initiative, Ben-Gurion University of the
49 Negev, Be'er Sheva, Israel
50

51 ⁸ University Lyon 1, Lyon, France
52

53 ⁹ Lyon Neuroscience Research Center, CRNL, INSERM, U1028, CNRS, UMR 5292,
54 Lyon, France
55
56
57
58
59
60

1
2
3 10 Institut des Sciences Cognitives Marc Jeannerod, CNRS, UMR 5229, Lyon, France
4

5 11 Instituto de Matemática Aplicada del Litoral, IMAL, CONICET-UNL, Santa Fe,
6 Argentina
7

8 12 Sorbonne Université, Paris Brain Institute (ICM), CNRS UMR722, INRIA Paris,
9 INSERM U1127, AP- HP Hôpital Pitié Salpêtrière, 75013, Paris, France
10

11 13 Chandra Family Department of Electrical and Computer Engineering, The University
12 of Texas at Austin, Austin, TX, 78712
13

14 14 Departments of Pediatrics and Clinical Neuroscience, Cumming School of Medicine,
15 University of Calgary
16

17 15 Data-Driven NeuroTechnology Lab, Donders Institute for Brain, Cognition and
18 Behaviour, Radboud University, Netherlands
19

20 16 School of Computer Science and Electronic Engineering, University of Essex,
21 Colchester, UK
22

23 17 Department of Radiology, University of Arkansas for Medical Sciences, Little Rock,
24 AR USA
25

26 18 Neurotechnology Group, Technische Universität Berlin, Berlin, Germany
27

28 19 BRAIN Center, University of Houston, Houston, USA
29

30 20 Italian Institute of Technology, University of Genoa
31

32 21 MIT Media Lab, Massachusetts Institute of Technology, Cambridge, USA
33

34 22 Department of Mechanical Engineering, Carnegie Mellon University
35

36 23 g.tec medical engineering GmbH, Schiedlberg, Austria
37

38 24 Rehab Neural Engineering Labs, Department of Physical Medicine and Rehabilitation,
39 University of Pittsburgh, Pittsburgh, PA, USA
40

41 25 Know-Center GmbH, Graz, Austria
42

43 26 BCI-NE, CSEE, University of Essex, Colchester, UK
44

45 27 Department of Neurosurgery, Faculty for Health, Medicine and Life Sciences,
46 Maastricht University, The Netherlands
47

48 28 Bernoulli Institute for Mathematics, Computer Science and Artificial Intelligence,
49 University of Groningen, The Netherlands
50

51 29 Univ. Bordeaux, CNRS, EPHE, INCIA, UMR5287 F-33000 Bordeaux
52

53 30 Mike Wieggers Department of Electrical and Computer Engineering, Kansas State
54 University, USA
55
56
57
58
59
60

1
2
3 ³¹ Italian Institute of Technology, via Morego 30, 16163 Genova, Italy
4

5 ³² Division of Biology and Biological Engineering, California Institute of Technology,
6 Pasadena, CA, USA
7

8 ³³ Department of Neurological Surgery, University of California, Davis, USA
9

10 ³⁴ BCI4Kids, Department of Pediatrics, University of Calgary, Calgary, Canada
11

12 ³⁵ Inria center at the university of Bordeaux / LaBRI, France
13

14 ³⁶ Ophthalmology Department, University of Pittsburgh, Pittsburgh, USA
15

16 ³⁷ Department of Biomedical Engineering, Fixel Institute for Neurological Diseases,
17 University of Florida, Gainesville, Florida, USA
18

19 ³⁸ National Center for Adaptive Neurotechnologies, Stratton VAMC, Albany, NY USA
20

21 ³⁹ Technogym UK, 2 The Blvd, Cain Rd, Bracknell RG12 1WP
22
23
24

25 Keywords: brain-computer interfaces, speech decoding, neurorehabilitation, sensory
26 restoration, sensorimotor cortex
27
28
29
30
31
32
33
34
35
36
37
38
39
40
41
42
43
44
45
46
47
48
49
50
51
52
53
54
55
56
57
58
59
60

Abstract

The Tenth International Brain-Computer Interface (BCI) Meeting was held June 6-9, 2023, in the Sonian Forest in Brussels, Belgium. At that meeting, 21 master classes, organized by the BCI Society's Postdoc & Student Committee, supported the Society's goal of fostering learning opportunities and meaningful interactions for trainees in BCI-related fields. Master classes provide an informal environment where senior researchers can give constructive feedback to the trainee on their chosen and specific pursuit. The topics of the master classes span the whole gamut of BCI research and techniques. These include data acquisition, neural decoding and analysis, invasive and noninvasive stimulation, and ethical and transitional considerations. Additionally, master classes spotlight innovations in BCI research. Herein, we discuss what was presented within the master classes by highlighting each trainee and expert researcher, providing relevant background information and results from each presentation, and summarizing discussion and references for further study.

1. Introduction

The Tenth International Brain-Computer Interface (BCI) Meeting provided a venue for trainees to present and receive feedback for their work in BCI. This paper is intended to highlight their work and the innovation occurring in BCI research.

1.1 Purpose and organization of master classes

The master classes were organized by the Postdoc & Student Committee of the BCI Society, whose primary goal is to foster learning and engagement opportunities for trainees. Trainees submitting abstracts to the BCI Meeting could opt if they would like to participate in master classes. Abstract selection is based on evaluations by the Program Committee, considering reviewers' scores, diversity, and inclusion. Trainees could submit their abstract under seven general themes including BCI implant - control, BCI implant - other, BCI non-implanted - control, BCI non-implanted - other, signal acquisition, signal analysis, and user aspects: experience, ethics, target populations. Out of 93 potential candidates for master classes, 42 trainees (45%) were selected. These trainees, along with 14 masters, were organized into 21 master classes. Of the 42 trainees, 34 were graduate students, 7 were postdoctoral fellows, and 1 was a medical student. Classes were held in seven parallel sessions on three separate days of the meeting.

The master classes are meant to promote opportunities for trainees to showcase their work and to encourage relaxed interactions with senior members of their field. The master class format is as follows: two BCI trainees present their work for 10-15 minutes and one senior researcher, or master, provides constructive feedback. Additionally, any participant of the BCI Meeting may attend a master class and take part in the discussion.

The summaries provided by the master class trainees in this paper create a convenient overview of the range of topics included in BCI research, and the challenges current BCI researchers face as they advance the technology and the field. We have divided the summaries into eight specific themes: speech decoding, motor imagery, BCIs for pediatric populations, platforms for closed-loop BCIs, deep learning applications, neurorehabilitation, sampling for sensorimotor BCIs, and novel BCI techniques for improved performance. For each summary, we report the trainee, the title of their

presentation, the initial theme, and the master assigned to each class, as shown in Table 1. Each summary introduces the trainee's presentation, their preliminary findings and their conclusions. Note, that 'we' within each summary refers to the trainee and their initial abstract submission co-authors.

Theme	Presenter	Master	Initial Theme	Title
Speech decoding	Julia Berezutskaya	Sergey Stavisky	Signal analysis	Optimizing feature selection for word decoding with high-density electrocorticography
	Richard Csaky	Christian Herff	Signal acquisition	Inner speech decoding from electroencephalography and magnetoencephalography
	Maxime Verwoert	Sergey Stavisky	Signal analysis	Evaluating implant locations for a minimally invasive speech BCI
Motor imagery BCIs	Daniel Polyakov	Christian Herff	Non-implanted – control	Recruiting neural field theory for motor imagery data augmentation
	Sotirios Papadopoulos	Richard Andersen	Signal analysis	What is the exact relationship between beta band activity and hand motor imagery?
	Valeria Spagnolo	Ning Jiang	Non-implanted – control	Towards co-adaptive BCI based on supervised domain adaptation: results in motor imagery simulated data
	Juliana Gonzalez Astudillo	Richard Andersen	Signal analysis	Network features for motor imagery-based brain-computer interfaces
	Satyam Kumar & Hussein Alawieh	Fabien Lotte	Non-implanted – control	Transfer Learning Promotes Acquisition of Individual BCI Skills
BCIs for pediatric populations	Dion Kelly	Camille Jeunet	User aspects	The effect of gamified calibration environments on P300 and MI BCI performance in children
	Joanna R.G. Keough	Camille Jeunet	User aspects	Mechanisms and Impacts of Brain-Computer Interface Fatigue in Children
	Araz Minhas	David E. Thompson	Non-implanted – other	Does my Child Know I'm Here? EEG Signatures of Parental Comfort for Disorders of Consciousness in a Critically Ill Child
Platforms for closed-loop BCI research	Matthias Dold	Aysegul Gunduz & Andreea Ioana Sburlea	Implanted – control	Platform for closed-loop deep brain stimulation research: DAREPLANE
Deep learning in BCIs	Yiyuan Han	Christian Herff	Signal analysis	Offline Prediction of Prolonged Acute Pain by means of Convolutional Neural Network Model applied to Electroencephalographic Oscillatory Connectivity
	Alexander McClanahan	Xing Chen	Signal analysis	Decoding Visual Scenes from Visual Cortex Spikes Using Deep Learning

	Mousa Mustafa	Marianna Semprini	Implanted – other	Decoding Invasive Brain Signals Using Deep Learning
Exploring BCIs for neurorehabilitation	Jose Gonzalez-Espana	Ning Jiang	Non-implanted – control	NeuroExo: A Low cost Non Invasive Brain Computer Interface for upper-limb stroke neurorehabilitation at home
	Florencia Garro	Ning Jiang	Non-implanted – control	Effects of Robotic Assistance in ERP Modulation for Upper-limb Exoskeleton Control
	Angela Vujic	David E. Thompson	Non-implanted – other	Joie: An Affective Brain-computer Interface for Learning Mental Strategies for Positive Affect
Advancements in sampling the sensorimotor cortex	Kriti Kacker	Richard Andersen	Implanted – control	Spectral features of endovascular ECoG signals recorded from a Stentrode in human motor cortex
	Christoph Kapeller	Christian Herff	Signal acquisition	Increased spatial resolution reveals separated EEG activation of individual finger movements
	Simon Geukes	Victoria Peterson	Signal analysis	Ultra-high-density electrocorticography recordings of the human sensorimotor cortex
Novel techniques for advancing BCI performance	Tan Gemicioglu	Ning Jiang	Non-implanted – control	Transitional Gestures for Enhancing ITR and Accuracy in Movement-based BCIs
	Ceci Verbaarschot	Marianna Semprini	Implanted – other	The effect of artificially created sensory feedback on motor cortex activity during task performance
	Michael Wimmer	Marianna Semprini	Non-implanted – other	Toward Hybrid BCI: EEG and Pupillometric Signatures of Error Perception in an Immersive Navigation Task in VR
	Mushfika Sultana	Eli Kinney-Lang	Non-implanted – other	Assessing the impact of transcranial Direct Current Stimulation on the enhancement of race driving skills
	Sara Ahmadi	Xing Chen	Signal analysis	A model-based dynamic stopping method for code-modulated visual evoked potentials BCI

Table 1. Summaries included in this paper and presented during the master classes, arranged by theme and following the same order as the sections.

2. Master class themes and summaries

2.1 Speech decoding

In recent years, there has been an influx of research focused on the potential use of BCIs as augmentative and alternative communication devices for patients with damage or degeneration of speech motor pathways [1,2]. Understanding optimal temporal and spatial neural recording resolution, advantages of different recording modalities (e.g.,

1
2
3 noninvasive or invasive) or decoding strategies are a few aspects that are critical to the
4 tailoring of speech BCIs for clinical populations. Additionally, there is increased interest
5 in decoding covert speech and discerning the fundamental differences between covert
6 and overt speech production [3].
7
8
9

10 **2.1.a. Presenter:** Julia Berezutskaya, PhD (University Medical Center, Utrecht,
11 Netherlands)
12

13
14
15 *Title:* Optimizing feature selection for word decoding with high-density
16 electrocorticography
17

18
19 *Master:* Sergey Stavisky, PhD (University of California, Davis, USA)
20

21 *Theme:* Signal analysis
22
23

24 High-accuracy individual word decoding from brain activity is crucial for the
25 development of speech BCIs for people who cannot speak due to paralysis [4]. Here, we
26 investigated a) how accurate word decoding is from brain signals obtained with high-
27 density electrocorticography (ECoG) grids, and b) what neural features are most
28 informative for high decoding performance. Five subjects participated in a word reading
29 experiment during which their brain activity was recorded with high-density ECoG. There
30 were 12 unique words, and each word was spoken aloud 10 times. ECoG signals in alpha
31 (8-12 Hz), beta (13-30 Hz) and high frequency band (HFB, 70-170 Hz) were
32 downsampled to 75 Hz and arranged into word trials using windows from 250 milliseconds
33 prior to word onset to the length of the longest pronounced word (about 1.1 second). We
34 used a support vector machine classifier with leave-one-out cross validation to test five
35 feature selection strategies: 1) all electrodes & alpha, beta, HFB; 2) a subgrid of 32
36 electrodes & alpha, beta, HFB; 3) all electrodes & HFB; 4) a subgrid of 32 electrodes &
37 HFB; 5) recursive feature elimination & alpha, beta, HFB.
38
39
40
41
42
43
44
45
46
47

48 The best performing algorithm (5) led to the accuracy of 98%, 87%, 67%, 98% and
49 59% for S1, S2, S3, S4 and S5, respectively (chance is 8%, Figure 1a). On average, this
50 accuracy was at least 20% higher compared to the default strategy of no feature selection
51 (1). HFB features were most informative for decoding. Electrodes that contributed to high
52
53
54
55
56
57
58
59
60

accuracy decoding the most were distributed along the ventral sensorimotor cortex (Figure 1b).

This work has several limitations. First, the dataset size was relatively small. Second, the data were collected from able-bodied participants. Both are consequences of doing research on temporary ECoG recordings in human subjects. Despite these limitations, our results offer a methodology for obtaining high-accuracy word decoding from brain activity while optimizing selection of frequency and electrode features. Maximizing individual word decoding performance this way has the potential to further advance the development of speech BCIs. Future work will focus on optimal feature selection in the time dimension with the aim to identify a time window in neural data that leads to best decoding. We will also extend this methodology to tasks other than word reading and release the toolbox for optimal neural feature selection for BCI decoding to the neuroscience community.

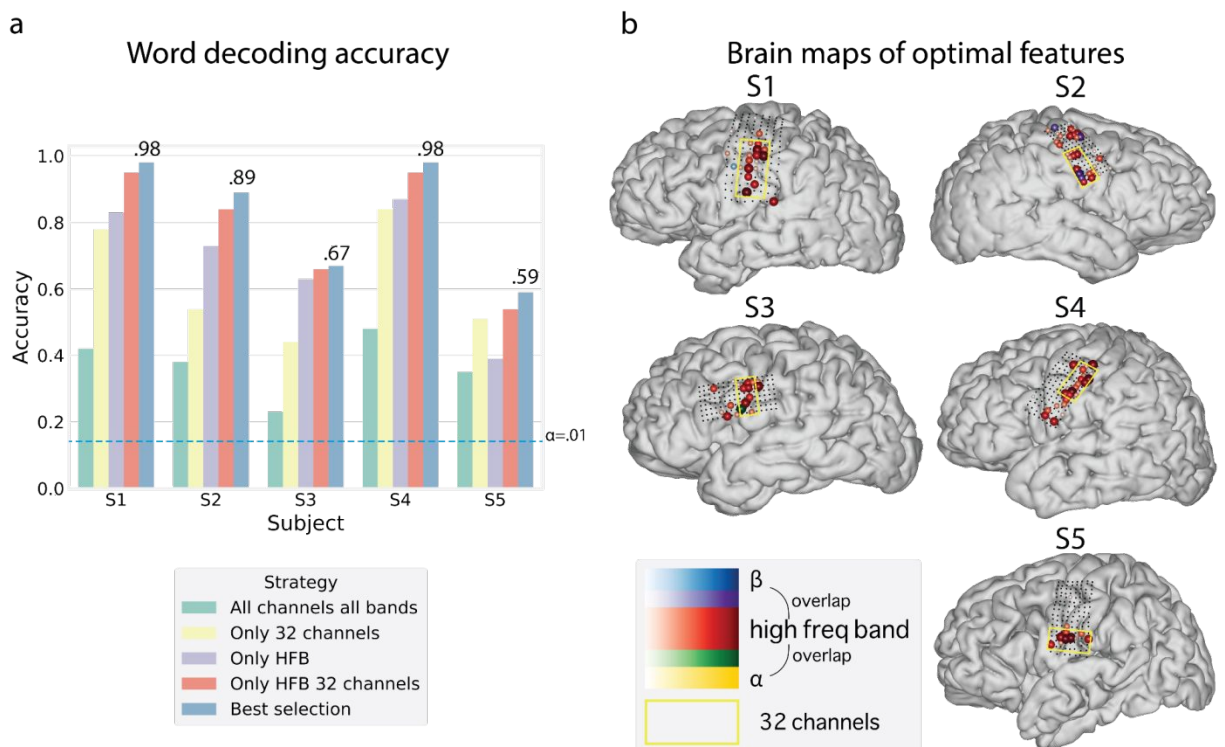


Figure 1. Optimal feature selection results. (a) Word decoding accuracy for five feature selection strategies. Chance level accuracy is shown with a dashed blue line. Since leave-one-

1
2
3 out cross-validation was used, no error bars are shown. (b) Optimal features identified with
4 strategy (5) are shown on individual subject brain renderings. For reference, optimal features
5 identified with strategy (2) are also shown suggesting that both a combinatorics approach
6 looking for the best smaller subgrid and a recursive feature elimination approach may provide
7 overlapping results. Colored electrodes represent electrodes chosen by recursive feature
8 elimination as optimal (color denotes the frequency range in which the electrode was chosen).
9
10
11
12

13 Small black electrodes outline the overall electrode grid coverage.

14
15 **2.1.b. Presenter:** Richard Csaky, PhD (University of Oxford, United Kingdom)

16
17 *Title:* Inner speech decoding from electroencephalography and
18 magnetoencephalography
19

20
21 *Master:* Christian Herff, PhD (Maastricht University, Netherlands)

22
23
24 *Theme:* Signal acquisition
25

26 Although inner speech is commonly experienced in daily life, there has been a
27 scarcity of research focusing on imaged or covert speech, especially regarding non-
28 invasive techniques [5]. This study seeks to address this gap by using
29 electroencephalography (EEG) and magnetoencephalography (MEG) to collect data
30 during three different inner speech paradigms, along with conducting an initial decoding
31 analysis. Such research has the potential to lay the groundwork for word-level
32 communication via brain-computer interfaces [6].
33
34
35
36
37

38 We conducted a study to examine the differences between silent reading,
39 repetitive inner speech, and generative inner speech using five patient-relevant words
40 (help, hungry, tired, pain, thirsty) in three healthy participants. Before and after each
41 session, 5 minutes of resting state EEG and MEG data were collected. For all sessions,
42 we additionally collected electrocardiography (ECG), electrooculogram (EOG),
43 electromyography (EMG; on the jaw), and eye-tracking data. We collected a large number
44 of inner speech trials (~200/word) in each session.
45
46
47
48
49

50 Although several methods were tried, no significant decoding was obtained using
51 the MEG inner speech data. On the silent reading trials, we trained a 2-layer linear neural
52 network using the entire 1-second epoch with 20-fold cross-validation. For one of the
53 participants with six sessions, 30% validation accuracy was obtained, whereas 44% was
54
55
56
57
58
59
60

1
2
3 achieved for the other participants (Figure 2 - example validation accuracy from one
4 participant). Using a sliding-window linear discriminant analysis model, the peak accuracy
5 was observed between 300 and 400 ms post-stimulus. In the EEG inner speech data, we
6 found above-chance validation accuracy in only 3 sessions (out of 10), with an average
7 of 25% in these 3 sessions. We tried various BCI decoding methods, e.g., wavelet
8 features, Riemannian classification, and linear and nonlinear models, but nothing seemed
9 to improve performance.
10
11
12
13
14

15 We explored the potential of decoding inner speech from a new MEG and EEG
16 dataset through three paradigms across a few participants, but with a large number of
17 trials. Our silent reading results demonstrate the feasibility of decoding visual
18 representations of words from non-invasive recordings. The decoding appeared to be
19 driven by early visual responses, with a later peak potentially reflecting higher-level
20 language processing. This late component merits further investigation as a marker of
21 semantic processing.
22
23
24
25
26
27

28 In contrast to silent reading, our extensive efforts to decode two types of inner
29 speech were largely unsuccessful across EEG and MEG. While we explored various
30 decoding algorithms and experimental designs, accuracy never substantially exceeded
31 chance levels. This contrasts with more promising results from intracranial recordings in
32 humans and suggests non-invasive signals may not adequately capture the subtle
33 dynamics of inner speech.
34
35
36
37
38

39 Several factors could underlie the difficulty of decoding inner speech non-
40 invasively. Inner speech lacks the external stimuli and muscle activations present during
41 overt tasks, reducing the signal-to-noise ratio. There is also high inter-individual variability
42 in inner speech strategies. Here we focused on collecting large trial counts from a few
43 participants rather than a small sample across many subjects. Further limitations of our
44 work include the small number of participants and the small set of words.
45
46
47
48
49
50

51 Future investigations could explore alternative paradigms more representative of
52 natural speech, such as imagining longer phrases or reading whole sentences silently.
53 Transfer learning and self-supervision may help extract robust inner speech
54
55
56
57
58
59
60

representations amidst noise. Intracranial findings point to superior temporal, inferior frontal, and motor areas as promising decoding targets. For non-invasive BCIs, approaches beyond word-level decoding may be needed for inner speech-based communication, such as decoding phonemes, or imagined handwriting.

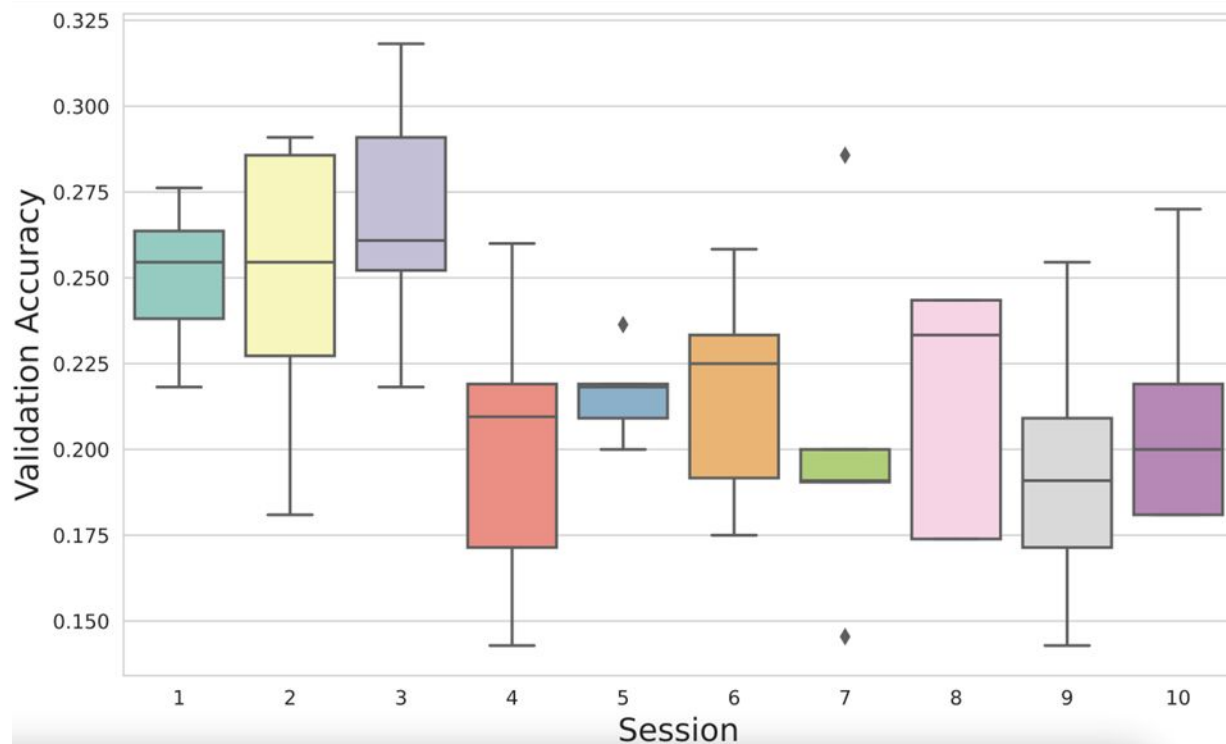


Figure 2. Validation accuracy distributions across the 5 folds of the 10 inner speech EEG sessions of one participant. Separate LDA models are trained and evaluated on each fold and session to decode which of the 5 words is being used in the 1-second inner speech trials. Chance level is 0.2.

2.1.c. Presenter: Maxime Verwoert (Maastricht University, Netherlands)

Title: Evaluating implant locations for a minimally invasive speech BCI

Master: Sergey Stavisky, PhD (University of California, Davis, USA)

Theme: Signal analysis

Speech BCIs present a promising avenue for restoring communication in individuals affected by a speech impairment, by converting neural signals into speech.

1
2
3 While conventional intracranial BCI technologies often necessitate craniotomies for
4 implantation, stereo-electroencephalography (sEEG) offers a less invasive option,
5 requiring only small burr holes [7]. This technology has the added benefit of sampling
6 many cortical and subcortical regions at once. With the brain-wide coverage obtained
7 through many recordings with epilepsy patients using sEEG electrodes, we sought to
8 determine suitable electrode shaft locations for a speech BCI.
9
10
11
12
13

14 We recorded overt speech production data with 24 participants. Their acoustic and
15 neural data were time-aligned before applying an electrode-shaft re-reference. A unit
16 selection approach was used to reconstruct the neural signal directly into audio using a
17 10-fold cross-validation. Each individual shaft of each participant was analyzed separately
18 to examine the spatial characteristics of decoding accuracy. We evaluated the audio
19 reconstruction performance for each shaft by correlating the spectrogram of the original
20 speech waveform to that of the reconstructed waveform.
21
22
23
24
25
26

27 Only a small number of shafts had a significant speech reconstruction performance
28 and were mostly located near the lateral and central sulci (Figure 3). The prefrontal and
29 occipital cortices did not appear to be informative. There was no difference in
30 performance between the two hemispheres. We identified five cortical regions, in addition
31 to many contacts in white matter, that were most involved in the significant shafts: the
32 auditory cortex, the superior temporal cortex, the pre- and postcentral cortices and the
33 insula. The insula, auditory cortex, other sulcal regions and contacts within white matter
34 are particularly interesting, as these are not usually sampled with electrodes on the
35 cortical surface. Identifying these target locations for a less invasive speech BCI may help
36 in developing an advantageous solution to restore communication for individuals with
37 speech impairments.
38
39
40
41
42
43
44
45
46
47
48
49
50
51
52
53
54
55
56
57
58
59
60

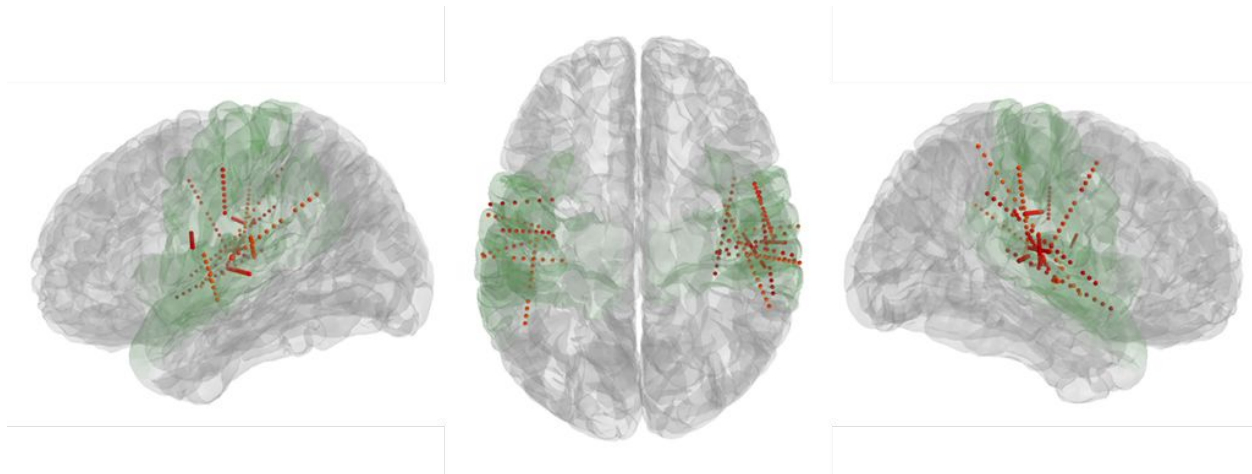


Figure 3. Electrode contacts belonging to significant shafts depicted in red, projected on an averaged brain. Highlighted in green are the most important regions (auditory cortex, superior temporal cortex, pre- and postcentral cortices, insula) in both hemispheres.

2.2 Motor imagery brain-computer interfaces

Motor imagery-based BCIs have been a common method throughout the history of BCI and are particularly popular for non-invasive approaches such as EEG [8]. Motor imagery has been convenient for a wide variety of patient populations and consumer applications alike, as it does not need external stimuli to perform and provides an intuitive mapping for control tasks. However, motor imagery often requires training for each user and can suffer from low accuracy when classifying multiple imagined movements. The recent work in this area pushes the boundaries of decoding by evaluating alternate features such as beta burst activity and novel motor network metrics to enhance classification. Researchers also attempt to reduce the data needed for motor imagery by applying domain adaptation, data augmentation techniques and transfer learning.

2.2.a. Presenter: Daniel Polyakov, PhD (Ben-Gurion University, Israel)

Title: Recruiting neural field theory for motor imagery data augmentation

Master: Christian Herff, PhD (Maastricht University, Netherlands)

Theme: BCI non-implanted - control

1
2
3 This study presents a new approach to enhance BCIs that rely on motor imagery
4 (MI). A common challenge faced by MI-based BCIs is the scarcity of diverse training data,
5 hindering their accuracy and practicality. To address this, we introduce a novel Data
6 Augmentation (DA) method leveraging Neural Field Theory (NFT), a computational model
7 inspired by the human brain's neural dynamics (Figure 4) [9].
8
9

10
11
12 The core innovation lies in using NFT to generate artificial EEG time series that
13 mimic the ones recorded during an MI task, in order to expand the training dataset. To
14 evaluate this approach, we employed the widely used '2a' dataset from BCI Competition
15 IV [10]. For each subject in the dataset, we fitted an NFT model to common spatial
16 patterns of each MI class, jittered the fitted parameters to enhance diversity, and
17 generated time series for DA.
18
19
20
21
22
23

24 Our method resulted in a significant accuracy improvement of over 2% when
25 classifying the "total power" feature, but it did not enhance classification for the "Higuchi
26 fractal dimension" (HFD) feature. We compared our approach with a DA method that adds
27 Gaussian noise to feature values, but the noise-based method failed to achieve
28 statistically significant accuracy improvements.
29
30
31
32

33 The lack of improvement in HFD-based classification suggests that the NFT model
34 was more effective at representing certain features, particularly those in the time domain.
35 This could be because the NFT fitting process discards phase information, potentially
36 limiting its effectiveness for features like HFD. Another finding was that user proficiency
37 in MI tasks influenced the efficacy of the DA, with more proficient users benefiting more
38 from the augmentation.
39
40
41
42
43
44

45 This study provides insights into the underlying mechanisms of the augmentation
46 process by examining how NFT parameters impact the extracted features. Future
47 research could explore the efficiency of this DA method for additional MI classification
48 features, such as kurtosis or sample entropy, with a focus on parameter jittering.
49 Additionally, assessing this method's compatibility with other BCI paradigms could offer
50 further valuable applications.
51
52
53
54
55
56
57
58
59
60

In conclusion, this research represents a significant advancement in the field of MI-based BCIs. By employing physiological models and innovative augmentation techniques, the study not only improves BCI performance but also offers valuable insights into the dynamics of neural field theory and its application in BCIs.

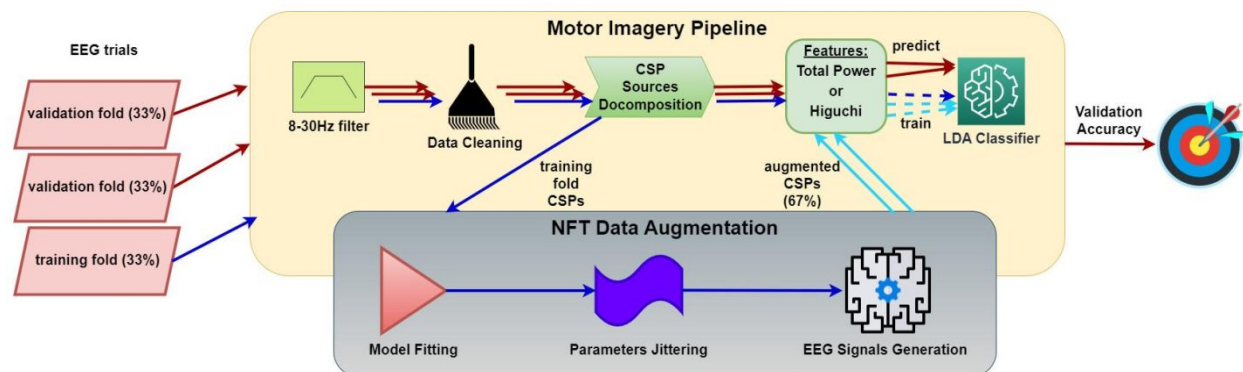


Figure 4. Evaluation workflow for MI data augmentation: A small dataset is created, and accuracy is tested using inverse cross-validation, with one-fold for training and the rest for testing. The motor imagery pipeline involves EEG preprocessing, common spatial pattern decomposition, feature extraction, and classification. NFT-based augmentation creates artificial CSP time series using a corticothalamic NFT model fitted to the original data. Reprinted from [11] with permission. EEG, electroencephalography; CSP, common spatial patterns; NFT, neural field theory; LDA, linear discriminant analysis

2.2.b. Presenter: Sotirios Papadopoulos (Université Claude Bernard Lyon 1, France)

Title: What is the exact relationship between beta band activity and hand motor imagery?

Master: Richard Andersen, PhD (California Institute of Technology, USA)

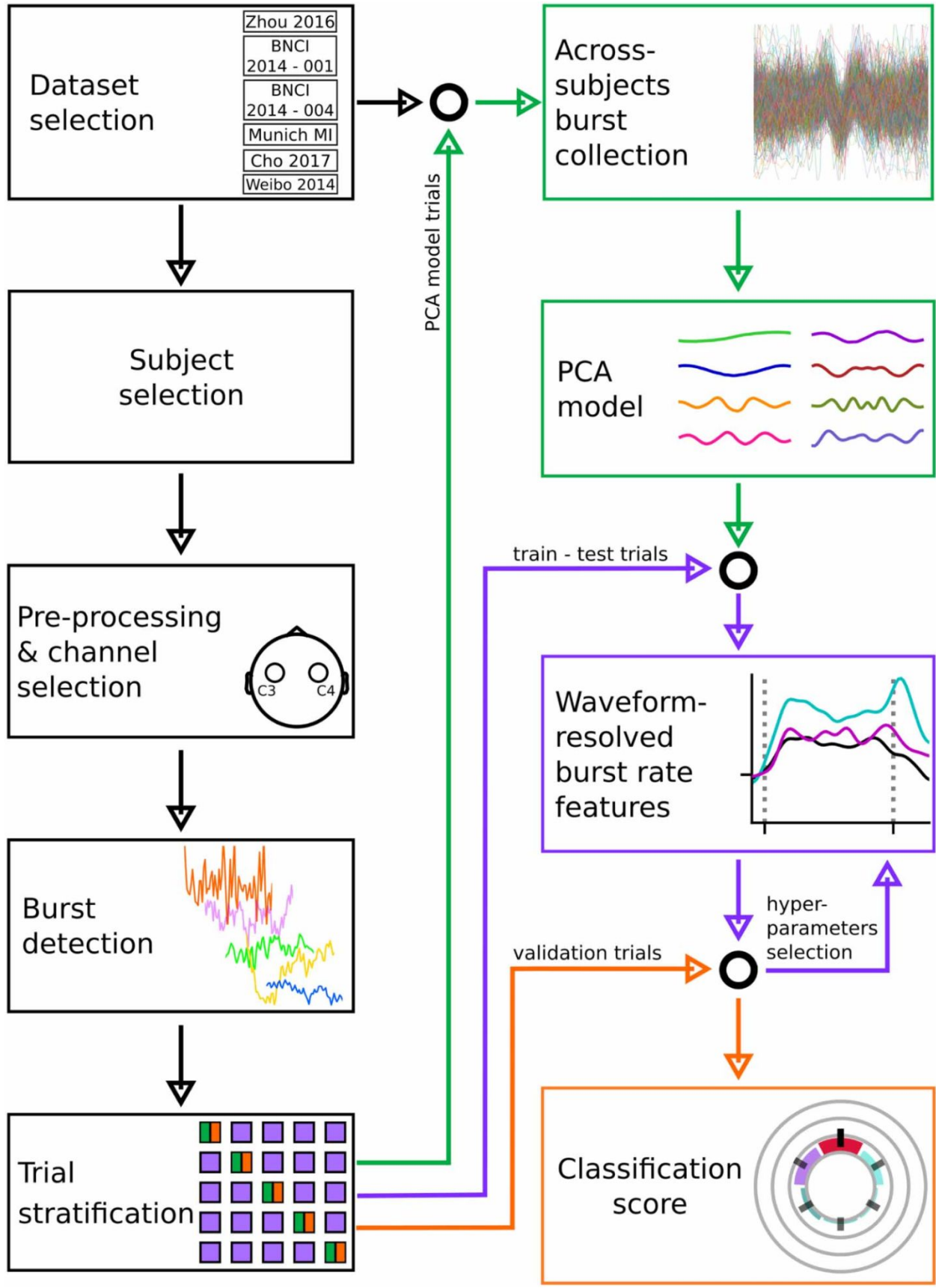
Theme: Signal analysis

Since the characterization of the event-related desynchronization (ERD) and synchronization (ERS) phenomena in the mu and beta frequency bands [12], the BCI community has heavily relied on band-limited power changes as the classification features of interest. Recent investigations in neuroscience have challenged the notion that signal power is the best descriptor of movement-related brain activity modulations,

1
2
3 particularly in the beta frequency band (~13-30 Hz). Studies have demonstrated that on
4 a single-trial level beta band activity occurs in short, transient events, termed “bursts”,
5 rather than sustained oscillations [13]. This suggests that the ERD/S patterns only
6 emerge when averaging across multiple trials, indicating that signal power may not fully
7 capture all relevant brain activity modulations during motor-related tasks.
8
9
10

11
12 Analyzing beta bursts holds promise for accessing markers that may be as
13 sensitive as beta power for classification, and that potentially capture more subtle
14 condition-specific changes. To investigate this possibility, we used six EEG datasets [14]
15 and examined the activity of channels C3 and C4 while the participants were performing
16 “left” and “right” hand motor imagery (MI). Using a new burst detection and waveform
17 analysis algorithm (Figure 5) [15], we demonstrated that classification features which
18 describe the modulation of burst rate for beta bursts with distinct waveforms can be more
19 informative than beta power alone. Furthermore, these features were more reliable than
20 conventional burst activity representations (e.g., rate, amplitude, temporal and frequency
21 spans). These results illuminate the non-linear relationship between beta burst activity
22 and band power, underscoring the potential benefit for the BCI field from incorporating
23 such recent neurophysiological findings [16].
24
25
26
27
28
29
30
31
32
33

34 In order to compute these waveform-specific burst rates, in this study we employed
35 a nested cross-validation classification procedure. The computational complexity of this
36 algorithm was a major limitation that needed to be circumvented so that a burst-based
37 analysis of the beta band activity could be suitable for BCI applications. To address this,
38 we took advantage of aforementioned results and in a follow-up study we introduced a
39 new framework for analyzing beta burst activity. Briefly, we defined a metric to identify
40 burst waveforms, recorded in channels C3 or C4, whose rate is expected to be maximally
41 modulated during a MI task. Then, we used these waveforms as data-driven kernels and
42 convolved the EEG recordings with each kernel. This allowed us to efficiently filter the
43 signals of all recording channels and gave us access to state-of-the-art classification
44 algorithms. We showed that beta burst waveforms, when used as data-driven filters, can
45 improve classification accuracy and information transfer rate [17], while also minimizing
46 the classification score loss in across-session transfer learning paradigms [18].
47
48
49
50
51
52
53
54
55
56
57
58
59
60



1
2
3
4
5
6
7
8
9
10
11
12
13
14
15
16
17
18
19
20
21
22
23
24
25
26
27
28
29
30
31
32
33
34
35
36
37
38
39
40
41
42
43
44
45
46
47
48
49
50
51
52
53
54
55
56
57
58
59
60

1
2
3 **Figure 5. Flowchart of the waveform-resolved burst rate analysis:** Each dataset was pre-
4 processed by rejecting trials and keeping channels C3 and C4. A burst detection algorithm was
5 applied to these raw signals. The remaining trials were split into three sets using nested 5-fold
6 cross-validation. The first set, used to sample bursts and create a principal component analysis
7 model (green boxes/arrows), combined data from all subjects. The second set, for
8 training/testing (purple boxes/arrows), selected the best waveform-resolved features via
9 repeated cross-validation. The third set (orange boxes/arrows) validated the model and
10 computed classification scores. Reprinted from [16] with permission. PCA, principal component
11 analysis.
12
13
14
15
16
17

18 **2.2.c. Presenter:** Valeria Spagnolo (Instituto de Matemática Aplicada del Litoral, IMAL,
19 CONICET-UNL, Santa Fe, Argentina)
20

21
22 *Title:* Towards co-adaptive BCI based on supervised domain adaptation: results in motor
23 imagery simulated data
24

25
26 *Master:* Ning Jiang, PhD (University of Waterloo, Canada)
27

28
29 *Theme:* BCI non-implanted - control
30

31 BCI can be thought of as a two-learners system, in which the user learns how to
32 control the computer and, simultaneously, the computer learns how to decode the user's
33 brain activity [19]. When used across several sessions, the machine learning system
34 employed to decode brain activity should adapt to changes in the EEG signal and help
35 the user in the development of stable brain patterns. In this line, a backward formulation
36 of optimal transport for domain adaptation (BOTDA) was proposed to avoid recalibration
37 in cross-session MI-BCIs and to improve decoding performance [20]. Although BOTDA
38 showed promising results in a supervised sample-wise scenario, it is interesting to
39 elucidate the extent to which the success of the adaptation depends on the subject's
40 ability to perform the MI task or on the adaptive capabilities of the model.
41
42
43
44
45
46
47
48

49 To investigate this, we simulated MI vs. rest EEG data to control MI alpha
50 desynchronization (i.e. ERD) in the left hemisphere during MI. We conducted different
51 cross-session scenarios, where a simulated session (S1) was used as a calibration
52 dataset and a second session (S2) was utilized for testing. For each session, 100 trials
53 of each class were generated. As a decoding algorithm, a common spatial pattern and a
54
55
56
57
58
59
60

1
2
3 linear discriminant analysis were used [21]. Firstly, the model was trained at the ideal
4 session (S1) and the performance of BOTDA was tested in sessions with decreasing
5 %ERD. BOTDA showed successful adaptation when the provided EEG patterns matched
6 the mental task, regardless of the %ERD in S2. On the contrary, experiments
7 manipulating the percentage of erroneous MI trials indicated that BOTDA could not
8 conduct a successful adaptation when there was a mismatch in between the provided
9 EEG pattern and the intended mental task. Finally, we trained the decoding model with
10 data from sessions with different ERD values. The decoder yielded chance-level
11 performance when calibration data lacked discernible ERD patterns, highlighting
12 BOTDA's efficacy only with discriminative calibration data. Results on these simulations
13 suggest that BOTDA can be a valuable tool for developing co-adaptive MI-BCI systems.
14
15
16
17
18
19
20
21
22

23 **2.2.d. Presenter:** Juliana Gonzalez Astudillo, PhD (Paris Brain Institute, France)

24
25 *Title:* Network features for motor imagery-based brain-computer interfaces

26
27
28 *Master:* Richard Andersen, PhD (California Institute of Technology, Pasadena, USA)

29
30
31 *Theme:* Signal analysis

32
33 Exploring the complexities of the brain's motor cortex has been a central focus in
34 neuroscience, particularly in advancing BCI technology. Traditionally, decoding MI has
35 relied on understanding the spatial organization of the motor cortex [22], known for its
36 principal involvement in controlling the contralateral side of the body. Moreover, recent
37 advancements underscore that functional connectivity patterns not only unveil this
38 lateralization during motor-related tasks but also offer a captivating window into modeling
39 MI as a dynamic and intricate network, where brain regions or sensors serve as nodes
40 and their statistical dependencies as links [23].
41
42
43
44
45

46 Here, we have investigated brain network topology and spatial organization's dual
47 contribution to enhancing MI decoding through functional lateralization [24]. Introducing
48 novel network metrics for *integration* (ω) and *segregation* (σ), we elucidate the
49 contributions of within- and across-hemispheric connections in modeling MI states.
50
51
52

53 Using multiple open-access datasets of EEG signals from MI experiments focusing on
54 left and right hand grasping motions [25], we construct spectral coherence-based
55
56
57
58
59
60

1
2
3 networks and calculate lateralization metrics for each electrode. Our analysis identifies
4 discriminant electrodes predominantly located in motor-related areas such as the primary
5 motor cortex, premotor area, supplementary motor area, and primary somatosensory
6 cortex, which are crucial for movement planning and execution. Notably, ω highlights
7 motor cortex involvement, while σ extends to frontal areas implicated in attention and
8 motor planning.
9

10
11 In BCI classification, these network properties yield competitive accuracy and
12 provide neurophysiological insights, contrasting with conventional approaches like
13 common spatial pattern filters and Riemannian methods, which lack neurophysiological
14 interpretation. However, the developed metrics are primarily suited for lateralized tasks,
15 for instance bilateral motor cortex recruitment may result in similar features for both
16 hands, limiting their discriminative power. Looking ahead, the precise detection of
17 involved areas opens up the possibility of analyzing the temporal dynamics of these
18 metrics to identify different stages of motor action. Combined with dynamic classification
19 techniques, this could provide a more accurate and reliable solution for BCI.
20
21
22
23
24
25
26
27
28
29

30 **2.2.e. Presenters:** Satyam Kumar & Hussein Alawieh (The University of Texas at Austin,
31 USA)

32 *Title:* Transfer Learning Promotes Acquisition of Individual BCI Skills

33
34
35
36 *Master:* Fabien Lotte, PhD (Inria Center at the University of Bordeaux, France)

37
38 *Theme:* BCI non-implanted - control
39

40
41 Motor imagery (MI) is one of the most commonly used modalities for controlling
42 BCIs [26–28] due to its volitional nature, requiring no external stimuli. However, MI-based
43 BCIs often necessitate tedious calibration sessions to record EEG data for building real-
44 time machine learning decoders, which may suboptimally perform due to inherent EEG
45 signal non-stationarity. Recent studies underlie the importance of longitudinal training with
46 closed-loop feedback for robust MI-BCI control [29,30]. In this study [31] we show that a
47 decoder trained on data from a single expert can provide consistent closed-loop feedback
48 to naive subjects thus promoting MI skill acquisition. We propose two subject-independent
49 real-time frameworks: a) Generic Recentering (GR) employing unsupervised domain
50
51
52
53
54
55
56
57
58
59
60

1
2
3 adaptation, and b) Personally Assisted Recentering (PAR), an extension of GR that
4 updates decoder parameters in real-time using a small amount of the naive subject data.
5 These frameworks are founded on Riemannian Geometry Classifiers, leveraging affine
6 invariant transforms to match covariate shifts on the Riemannian manifold [32,33],
7 thereby reducing non-stationarities in real-time and providing contingent closed-loop
8 feedback.
9
10
11
12
13

14 We tested our proposed framework on 18 BCI-naive volunteers, dividing them into
15 PAR and GR groups. Over five consecutive online training sessions, participants
16 controlled a standard binary class MI task with bar feedback [34] followed by a car racing
17 task [35]. Experimental results show that participants in both groups exhibited increases
18 in command delivery performance in the bar task (GR: $p < 0.05$ and PAR: $p < 0.01$).
19 Moreover, subjects show a significantly increasing trend in command delivery
20 performance over online sessions in both the frameworks. Race completion time values
21 in the car racing task indicated that participants could finish the races significantly faster
22 following the training sessions compared to their initial performance for both GR ($p < 0.01$)
23 and PAR ($p < 0.05$). Furthermore, feature separability analysis [36] showed significant
24 increasingly discriminant features for both frameworks and tasks. For both frameworks,
25 the most contributing EEG channels for discriminating between the two MI classes were
26 predominantly over the motor cortex. Despite using feedback from subject-independent
27 decoders, participants developed their own enhanced individual MI features, distinct from
28 the expert's data used for decoding. Finally, we demonstrate that unsupervised
29 adaptation (GR) coupled with longitudinal training reached statistically similar
30 performance to supervised recalibration (PAR) in a realistic setting.
31
32
33
34
35
36
37
38
39
40
41
42
43

44 Our proposed transfer learning frameworks promoted MI skill acquisition,
45 removing the need for calibration sessions. Participants demonstrated improved BCI
46 control and increased feature discriminability over multiple training days, crucial for
47 mutual learning settings. Importantly, our frameworks enabled participants to modulate
48 their task-specific individualized feature spaces for BCI control, diverging from the
49 expert's patterns.
50
51
52
53
54
55
56
57
58
59
60

1
2
3 A limitation of the current work is that users operated the BCIs in binary class
4 settings. Future work should aim towards validating the proposed frameworks in
5 multiclass BCI settings to enhance the degree of freedom for controlling external devices
6 and applications. Moreover, the current study used data from a single expert subject for
7 online feedback. In the future, data from multiple experts could be pooled together to train
8 data-driven deep learning models like EEGNet [37] and TSMnet [38] for improving online
9 BCI feedback. Finally, these expert-based decoding frameworks could be used to provide
10 online feedback to stroke patients for longitudinal MI-BCI training who may struggle to
11 generate distinctive calibration data due to their reduced ability to modulate sensorimotor
12 rhythm [39].
13
14
15
16
17
18
19
20

21 **2.3 Brain-computer interfaces for pediatric populations**

22

23 BCIs hold promise for enhancing the interaction and communication abilities of individuals
24 with motor impairments. However, there has been limited exploration of BCI research
25 involving pediatric and young adult populations [40]. Existing studies in these
26 demographics have yielded conflicting results, underscoring the need for the BCI
27 community to focus on enhancing the design, implementation, and user experience
28 specifically tailored for pediatric and young adult populations. This emphasis is especially
29 crucial for individuals with neurodevelopmental disorders, neurodegenerative disorders,
30 or severe motor disabilities.
31
32
33
34
35
36
37

38 **2.3.a. Presenter:** Dion Kelly, PhD (University of Calgary, Canada)

39
40 *Title:* The effect of gamified calibration environments on P300 and MI BCI performance
41 in children
42
43

44 *Master:* Camille Jeunet, PhD (Aquitaine Institute for Cognitive and Integrative
45 Neuroscience, Bordeaux, France)
46
47

48 *Theme:* User aspects: experience, ethics, target population
49
50

51 This study explored the potential of gamification to improve BCI calibration in
52 children, aiming to address longstanding calibration challenges such as monotony and
53 lack of engagement, which are exacerbated by children's limited attention and motivation
54
55
56
57
58
59
60

1
2
3 [41]. Incorporating scoring and rewards into calibration tasks, this randomized, cross-over
4 study compared gamified and non-gamified environments to assess their impact on
5 classification accuracy and task performance.
6
7

8
9
10
11
12
13
14
15
16
17
18
19
20
21
22
23
24
25
26
27
28
29
30
31
32
33
34
35
36
37
38
39
40
41
42
43
44
45
46
47
48
49
50
51
52
53
54
55
56
57
58
59
60

Thirty-two typically developing children (mean age 11.9 years) participated in two sessions, performing utility-driven tasks following gamified and non-gamified calibration. The tasks included spelling via visual P300 event-related potentials (Figure 6) and controlling a cursor via sensorimotor rhythm (SMR) modulation (Figure 7). Gamification elements like stories, quests, points, and sounds were integrated into the gamified calibration environments to enrich engagement. We evaluated BCI performance, including classification accuracy and online accuracy, as well as motivation, tolerability, and mental workload. For the P300 paradigm, classification accuracy was high in both gamified and non-gamified conditions, exceeding 96%. However, online performance during the spelling task was significantly lower following gamified calibration (71.47%) compared to non-gamified calibration (80.47%, $p < 0.01$). In the SMR paradigm, classification accuracy was 61.81% in the gamified condition versus 59.84% in the non-gamified condition, with no significant differences between conditions for classification or online cursor control performance. Furthermore, gamification did not significantly impact participants' motivation, tolerability, or workload perceptions.

This study highlights the capability of children to effectively use advanced BCI systems, achieving performance comparable to adults. However, the results suggest that the gamified elements employed may not have been sufficiently engaging. Several limitations should be noted, including the potential introduction of an auditory P300 component due to auditory stimuli in the gamified calibration task, which was absent in the utility-driven tasks and may have affected classification performance. Additionally, a ceiling effect in the P300 paradigm, where performance was already high in the non-gamified condition, may have limited the ability to observe the true impact of gamification on BCI performance.

Future investigations should focus on optimizing gamified calibration environments tailored to individual preferences and abilities. There is also a need to explore alternative gamification designs, potentially incorporating user feedback to enhance engagement

and motivation, especially for younger children or those with disabilities. Further research is also necessary to examine the long-term effects of repeated practice on BCI performance and to investigate how these results translate to clinical populations with motor impairments or communication challenges.



Figure 6. P300 scenes: standard calibration scene (left), gamified calibration scene (Mole Patrol game, middle), two-stage T9 speller scene for spelling task (right).

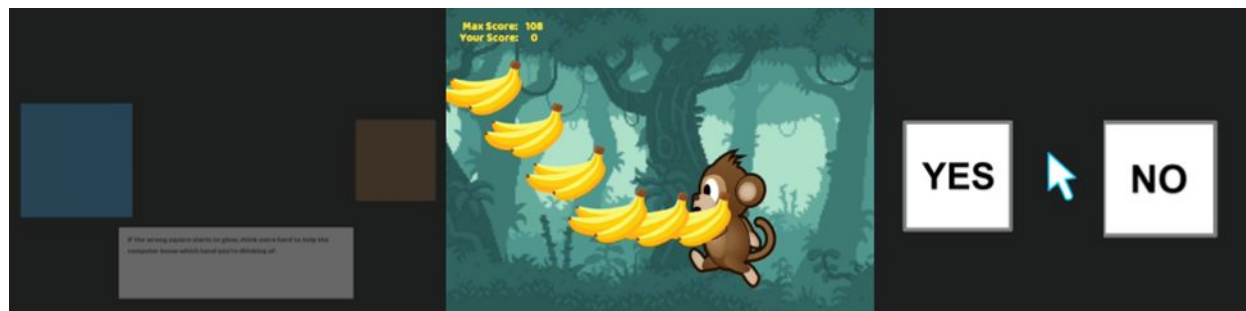


Figure 7. SMR scenes: standard calibration scene (left), gamified calibration scene (Banana Dash game, middle), cursor control scene for yes/no response task (right). Calibration consisted of 20 segments of six 1.5s-epochs for a total time of 5.67 minutes.

2.3.b. Presenter: Joanna R.G. Keough, MSc (University of Calgary, Canada)

Title: Mechanisms and Impacts of Brain-Computer Interface Fatigue in Children

Master: Camille Jeunet, PhD (Aquitaine Institute for Cognitive and Integrative Neuroscience, France)

1
2
3 *Theme:* User aspects: experience, ethics, target population
4

5
6 BCI can assist children with disabilities in communication, environmental
7 exploration, and gameplay [42]. BCI research is rapidly developing but has neglected
8 pediatric populations. Like many cognitively demanding tasks, fatigue is a critical factor
9 to consider for BCI performance and enjoyment [40] and has often been reported by
10 patients and families within our pediatric clinical BCI program. BCI fatigue has been
11 studied in adult populations, but there are no pediatric studies to date. This prospective,
12 cross over study assessed the effects of two BCI paradigms and a control condition on
13 self-reported fatigue and EEG biomarker of fatigue – alpha band power.
14
15
16
17
18
19

20 Thirty-two typically developing children aged 7-16 years participated in three
21 sessions: motor imagery-BCI, P300-BCI, and film viewing (control) (Figure 8). The DSI-
22 24C headset was utilized for BCI operation and EEG collection. Self-reported fatigue and
23 resting-state EEG alpha band power significantly increased across all sessions ($p < 0.001$;
24 $p = 0.047$ respectively). The increase in self-reported fatigue observed was greater in the
25 younger half of participants. These two measures of fatigue were uncorrelated to one
26 another. No differences in fatigue development between sessions were observed. This
27 project provides a baseline understanding of pediatric BCI fatigue. Short periods (30-
28 minutes) of BCI use can increase self-reported fatigue and an EEG biomarker of fatigue.
29 Performance was stable across BCI sessions and not associated with our measures of
30 fatigue.
31
32
33
34
35
36
37
38
39

40 The clinical implications and impact of fatigue on useability and enjoyment are
41 unclear and point to limitations of this study. These include a modest sample size and
42 large age range complicating age-based analysis. An additional unexpected challenge
43 was the tolerability of the DSI headset. Many participants found it uncomfortable and 25%
44 of participants requested to stop at least one of the three sessions early due to discomfort.
45 Despite these limitations, our results support the variability of fatigue and the overall BCI
46 experience in children that warrant future investigation to inform the design of pediatric
47 BCI systems to meet the unique goals of children and families. These investigations
48 should include longer BCI sessions with a more tolerable headset. Not all children had
49
50
51
52
53
54
55
56
57
58
59
60

adequate control of the BCI, and future work should uncover predictors of performance particularly in children. Strategies should be identified to promote BCI learning.

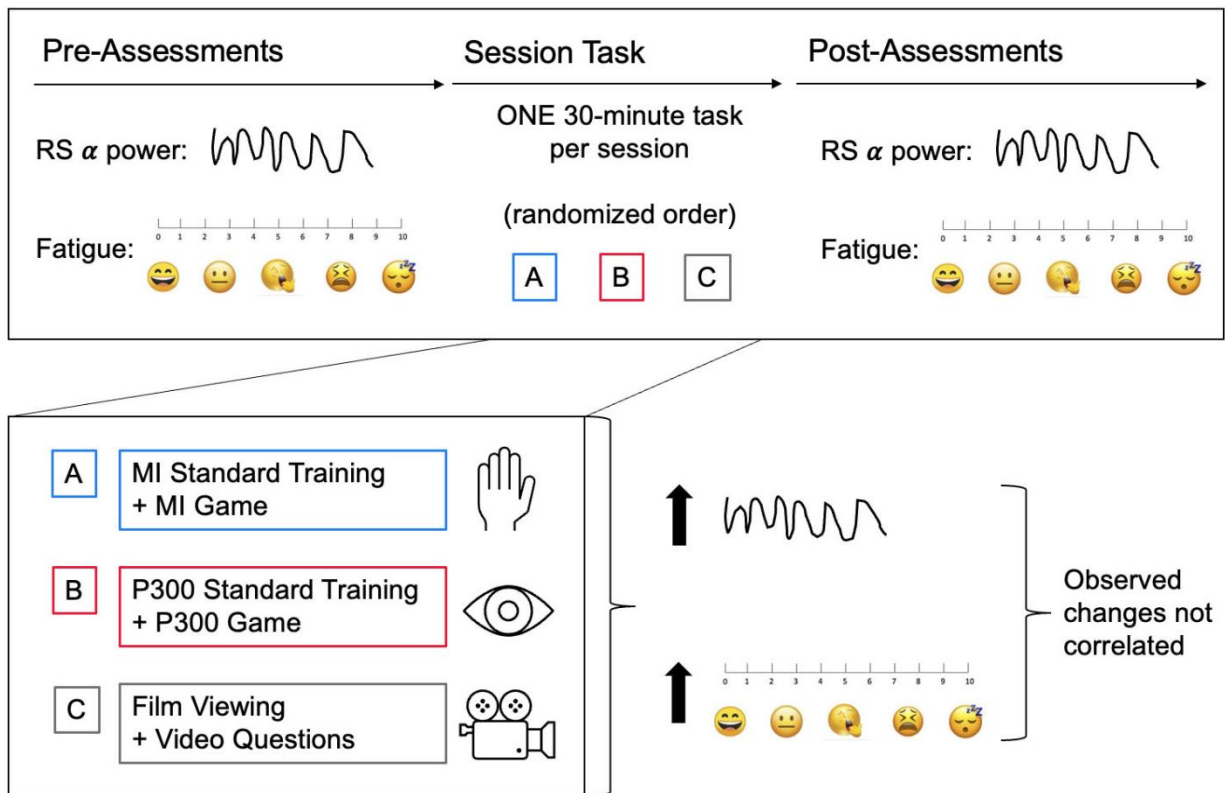


Figure 8. Protocol Schematic for All Three Sessions. Session tasks were balanced using a Latin square design. Sessions lasted 60 to 90 min. MI, motor imagery; RS, resting state.

Adapted with permission from figures originally published in [43].

2.3.c. *Presenter:* Araz Minhas (University of Calgary, Canada)

Title: Does my Child Know I'm Here? EEG Signatures of Parental Comfort for Disorders of Consciousness in a Critically Ill Child

Master: David E. Thompson, PhD (Kansas State University, USA)

Theme: BCI non-implanted - other

Each day in the Pediatric Intensive Care Unit (PICU), there are unconscious and comatose children afflicted with severe brain diseases, whose parents lie beside them, desperately wondering if their child will ever awaken. Up to 20% of adult patients with such disorders of consciousness (DoC) exhibit signs of cognitive-motor dissociation

1
2
3 (CMD) [44], wherein patients' willful modulation of brain activity may be observed via EEG
4 when given motor commands— indicating some intact cognition, despite behavioral
5 unresponsiveness. CMD is a promising early positive prognostic marker and may enable
6 some simple communication (“Yes”/ “No”) via BCIs for such patients. Unfortunately,
7 children have been largely neglected in CMD and BCI research [45]. However, much
8 potential for revealing CMD may lie in their developing brain networks' heightened
9 receptivity to social stimuli like parental comfort and affection. Detecting such networks'
10 activation in comatose children whose parents are constantly caring for them in the PICU
11 could reveal new brain activity markers that may help predict outcomes early and allow
12 families to communicate with their children in critical circumstances.
13
14
15
16
17
18
19

20 To explore this possibility, a 13-year-old female post-anoxic coma patient's 20-
21 channel EEG was analyzed with synchronized 17-hour PICU video footage. Highcuhi
22 Fractal Dimension values (HFD; indexing EEG complexity) were compared across video-
23 derived timestamps of parental comfort (physical contact / talking to children), presence
24 (in room), and absence. Shifts in child EEG complexity (mean HFD) positively correlated
25 with parental comfort ($r \approx 0.26$). HFD values formed two clusters (K-means;
26 Silhouette=0.54)— a higher HFD cluster (1.40 ± 0.11) coinciding mainly with parental
27 presence (74% of clustered time points), and one with lower HFD (1.24 ± 0.05) primarily
28 during parental absence (61%, $p < 0.01$). These preliminary results, summarized in Figure
29 9, suggest that parental comfort may elicit discernible EEG changes in pediatric DoC –
30 encouraging future investigations of such indicators for assisting prognosis or
31 communicative BCIs. As the generalizability of these results is limited by the single-
32 patient case design, future research involving larger cohorts will also be needed to
33 validate these findings, and more extensively explore the integration of such complexity
34 measures into prognostic models and potential BCI tools for pediatric coma.
35
36
37
38
39
40
41
42
43
44
45
46
47
48
49
50
51
52
53
54
55
56
57
58
59
60

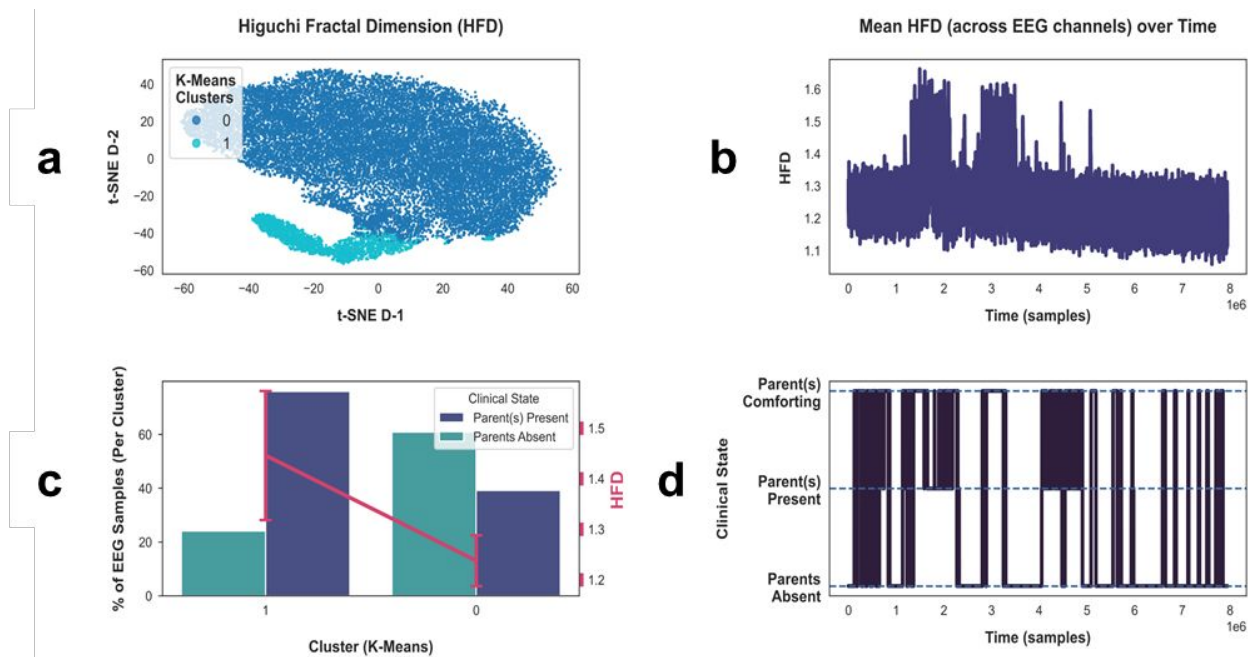


Figure 9. (a) K-means clustering of Higuchi Fractal Dimension (HFD) values from continuously recorded EEG (cEEG) data of a pediatric post-anoxic coma patient, revealing two distinct clusters. (b/d) Mean HFD values across channels over time, indicating fluctuations in EEG complexity. Temporal alignment of parental state with cEEG suggests a correlation between parental comfort and increased EEG complexity. (c) Distribution of EEG samples per cluster found higher HFD values associated with parental presence/comfort, and lower HFD during parental absence. Reprinted from [46] with permission.

2.4 Platforms for closed-loop brain-computer interface research

Closed-loop BCI applications encompass a diverse array of functionalities, extending from delivering precisely timed brain stimulation [47,48] to offering instantaneous feedback to users and facilitating the control of various end effectors [49]. This multifaceted scope enables closed-loop BCIs to cater to a wide spectrum of needs and scenarios, including therapeutic interventions, neurorehabilitation programs, and assistive technologies aimed at enhancing users' autonomy and quality of life. Developing platforms that can easily perform or integrate closed-loop applications may enable the generalizability and translation of these applications.

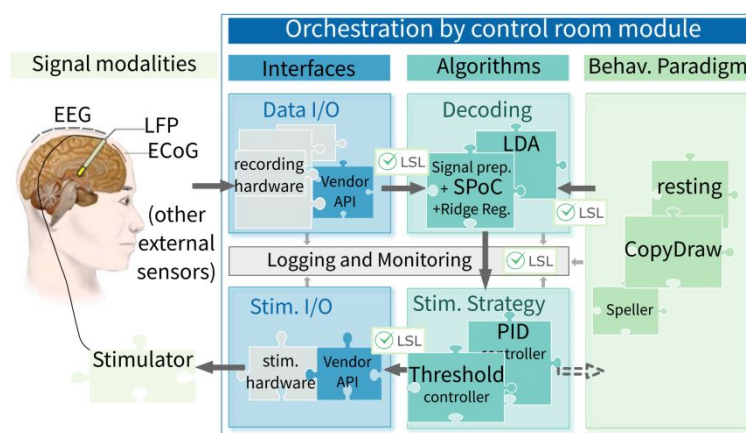
1
2
3 **2.4.a. Presenter:** Matthias Dold (Radboud University, Netherlands)
4

5 *Title:* Platform for closed-loop deep brain stimulation research: DAREPLANE
6

7
8 *Masters:* Aysegul Gunduz, PhD (University of Florida, USA) & Andreea Ioana Sburlea,
9 PhD (University of Groningen, Netherlands)
10

11 *Theme:* BCI implant - control
12
13

14
15 BCI continuously decode the brain state, a highly relevant building block for
16 adaptive neurostimulation. The **DA**ta driven **RE**search **PL**atform for **NE**urotechnology
17 (DAREPLANE) [50] project creates a modular open source platform to enable BCI
18 methods for adaptive closed-loop deep brain stimulation (aDBS). Current research on
19 aDBS is either conducted with custom soft- and hardware setups [51–53], or is fully
20 embedded in a single vendor's systems [54–56]. DAREPLANE supports customized
21 setups by providing a platform of open-source single responsibility modules for tasks
22 involved in closed-loop setups. Examples of such tasks related to aDBS are controlling
23 the stimulation parameters, decoding multi-modal recordings, exploring control
24 strategies, rendering of different user tasks, a thorough logging, and real time data
25 monitoring. An abstract high-level overview of such a setup with DAREPLANE is shown
26 in Figure 10.
27
28
29
30
31
32
33
34



49 **Figure 10.** Schematic of a closed-loop DBS experiment and involved DAREPLANE modules.
50 The jigsaw puzzle pieces represent different modules that can be combined to an aDBS setup.
51 Different modules for the same type of task can be switched in place. Adapted with permission
52 from [50]. EEG, electroencephalography; LFP, local field potential; ECoG, electrocorticography;
53 I/O, input/output; API, application programming interface; PID, proportional - integral - derivative
54
55
56
57
58
59
60

1
2
3
4
5 The platform is built with the experience of our previous work on decoding of neural
6 markers for deep brain stimulation (DBS) [53]. It relies on socket communication and uses
7 the lab streaming layer [57] protocol for data streaming. This choice makes it mostly
8 technology agnostic, with the exception of the central orchestration which is implemented
9 in Python. The modules can still be used standalone, relaxing the requirements to the
10 programming language the modules are implemented in.
11
12
13
14

15 An early stage version of the platform has already been used during a single aDBS
16 session and various open-loop DBS [50] in patients with Parkinson's disease (PD) while
17 they are performing a motor task [58]. Although targeted for aDBS experiments,
18 DAREPLANE can also be used to implement classical BCI applications like spellers or
19 motor-imagery controls. Due to the use of network communication, the bandwidth of the
20 involved network hardware can limit the throughput of the platform. This can be relevant
21 for high channel counts, with high sampling rates and depends on how much data is
22 shared between modules. Further work will investigate and quantify these limits in more
23 detail.
24
25
26
27
28
29
30

31 **2.5 Deep learning in brain-computer interfaces**

32
33 As the availability of large-scale datasets continues to grow, leveraging deep learning
34 techniques for feature extraction and decoding brain states within BCI systems holds the
35 potential to significantly enhance performance [59]. This advancement could lead to more
36 accurate and reliable outcomes, ultimately empowering BCI technology to better serve
37 individuals with diverse neurological conditions and needs.
38
39
40
41
42

43 **2.5.a. Presenter:** Yiyuan Han, PhD (University of Essex, United Kingdom)

44
45 *Title:* Offline Prediction of Prolonged Acute Pain by means of Convolutional Neural
46 Network Model applied to Electroencephalographic Oscillatory Connectivity
47
48

49 *Master:* Christian Herff, PhD (Maastricht University, Netherlands)

50
51
52 *Theme:* Signal analysis
53
54
55
56
57
58
59
60

1
2
3 Unresponsive patients, e.g., ones with disorder of consciousness, face challenges
4 in communicating their pain, making pain assessment difficult for caretakers. EEG signals
5 offer a potential avenue for pain assessment at the bedside. However, due to individual
6 variation, building accurate pain assessment models necessitates labeled data, which
7 cannot be obtained from unresponsive patients. To address this gap, we aimed to develop
8 a model capable of generalizing to new individuals without labeled data. For this purpose,
9 we trained a convolutional neural network (CNN) to classify pain and non-pain conditions
10 from EEG signals across individuals.
11
12

13
14
15
16
17 Forty-three healthy individuals participated in the experiment, with data from thirty-
18 six participants included for analysis after exclusions. We focused on two conditions: pain
19 induced by hot water (H) and resting states with eyes open (O) or closed (C). EEG signals
20 were segmented into 5-second trials with a 50% overlap. Inter-site phase clustering
21 (ISPC) was computed to measure functional connectivity between 32 EEG channels [60].
22 The ISPCs were reorganized into a 32x32 matrix as input features for the CNN model.
23 Leave-one-out tests were conducted for each participant, with one participant excluded
24 from model training. Cumulative evidence (CE) was computed to evaluate the effect of
25 the number of consecutive trials. In the binary classifications between pain condition (H)
26 and resting states (O or C), the accuracy of CE was significantly higher than the tests
27 without cumulative evidence within one minute (Figure 11a). For H vs O, the maximum
28 CE accuracy was $69.26\% \pm 14.72\%$, while the original accuracy was $63.99\% \pm 13.11\%$. For
29 H vs C, the maximum CE accuracy was $81.93\% \pm 14.73\%$ and the original accuracy was
30 $76.80\% \pm 15.28\%$.
31
32
33
34
35
36
37
38
39
40

41 For interpreting the model's generalization, we used Gradient-weighted Class
42 Activation Mapping (Grad-CAM) to generate the activation patterns of the functional
43 connectivity in binary classification (Figure 11b). Comparing the patterns for the binary
44 classification between H and O/C conditions, the functional connectivity between frontal
45 and central regions was specific to pain. The neurophysiology of somatic pain involves
46 the integration between frontal and central lobes, which might be the origin of such
47 specificity [61].
48
49
50
51
52

53 Individual variation in neural responses to pain poses challenges for pain
54 assessment model generalization. Transfer learning models are rare due to this variability
55
56
57
58
59
60

1
2
3 [62]. Recent research suggests that slow alpha frequency and alpha band functional
4 connectivity correlate with individual pain sensitivity, offering potential neural markers for
5 pain prediction [60,63]. Our study demonstrates the potential of alpha band functional
6 connectivity to mitigate individual differences in pain prediction, indicating a promising
7 avenue for future research in pain assessment using EEG signals. The analysis of
8 activation patterns suggested the interpretation of the obstacle in generalization,
9 Salomons revealed that prefrontal cortex activation is associated with individual
10 differences of pain perception [64]. Hence, the overlap of the frontal region in both pain-
11 related and individual-related specificity could harden the generalization.
12
13
14
15
16
17
18
19

20 This research did not effectively involve processing individual differences of neural
21 responses to pain, for example, transfer learning frameworks taking the individual-specific
22 feature into account. In the following study, we will develop transfer learning models to
23 improve the generalisability of the pain prediction model. Another limitation is that this
24 study did not consider the influences of thermoception, for which the innocuous thermal
25 stimulation can help declare its effects in the future.
26
27
28
29
30
31
32
33
34
35
36
37
38
39
40
41
42
43
44
45
46
47
48
49
50
51
52
53
54
55
56
57
58
59
60

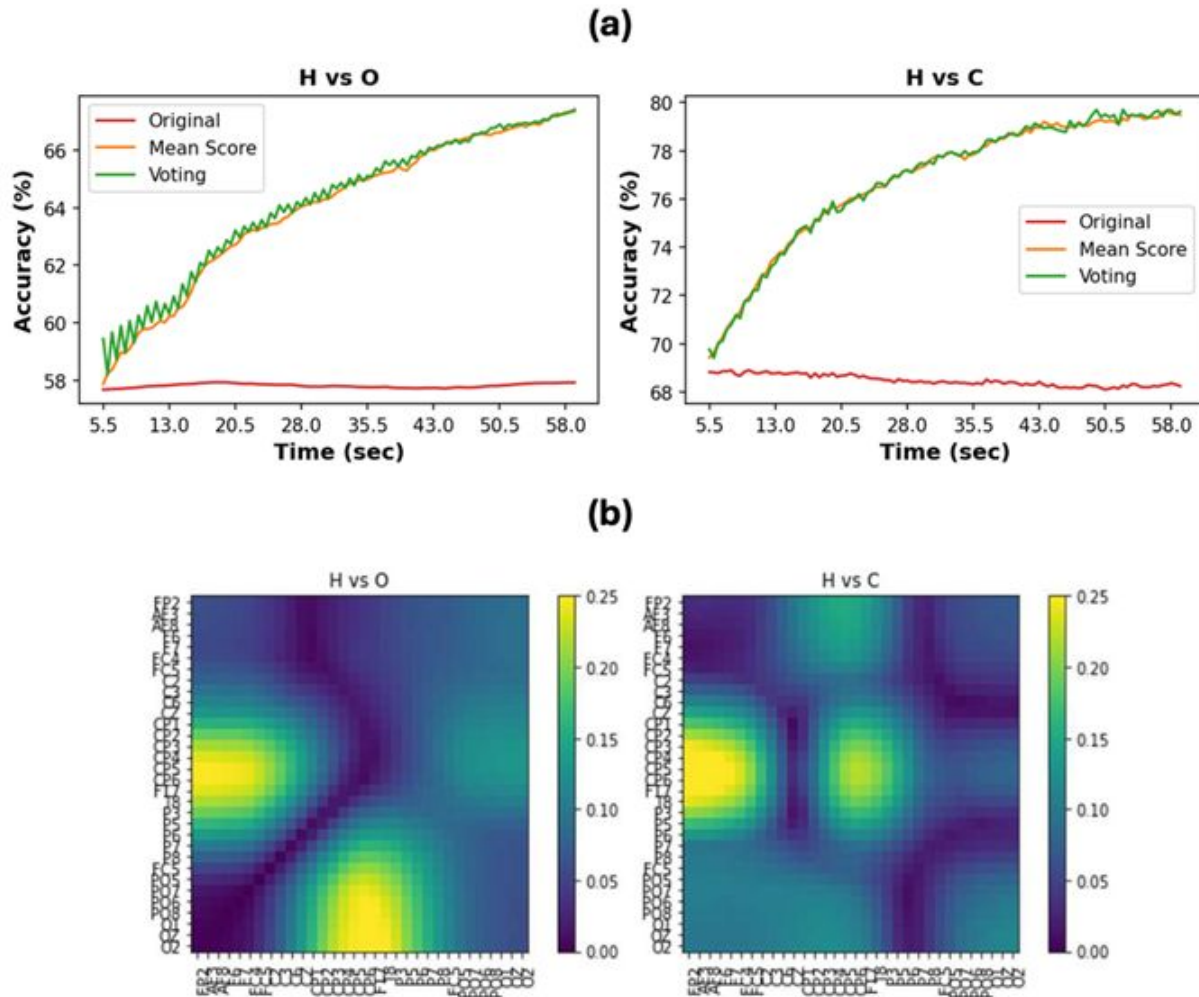


Figure 11. (a) The effect of time length to classification accuracy. The 'original' model represents the general evaluation without cumulative evidence, 'mean score' was based on the mean prediction score to predict the labels, and 'voting' mode predicted the labels according to the most frequency prediction in the cumulation range. Adapted from [65] with permission. (b)

Activation patterns of functional connectivity out of Grad-CAM. The highlighted regions represent the connectivity with higher weights in the classification. Adapted from [60] with permission.

2.5.b. Presenter: Alexander McClanahan, MD (University of Arkansas for Medical Sciences, USA)

Title: Decoding Visual Scenes from Visual Cortex Spikes Using Deep Learning

1
2
3 *Master:* Xing Chen, PhD (University of Pittsburgh, USA)
4

5
6 *Theme:* Signal analysis
7

8 Recent advancements in machine learning have revolutionized neural decoding,
9 showcasing remarkable achievements such as decoding rodent spatial coordinates via
10 hippocampal place cells, and motor activity [66,67]. We investigated the potential of deep
11 learning in decoding visual image stimuli from neural spikes across various time bins and
12 brain regions of the rodent brain.
13
14
15

16
17 Electrophysiology recordings and stimulus presentations were obtained from the
18 Allen Institute for Brain Sciences Visual Coding Neuropixels Dataset using the AllenSDK.
19 Three deep learning models were trained on spike counts across thousands of cortical
20 and subcortical neurons and over 5,000 natural scene stimulus presentations. Models
21 were tested on held-out test spikes and evaluated for image decoding accuracy.
22
23
24
25
26

27 Three machine learning models were trained to decode and classify which image
28 was shown to the animal solely from visual neural spiking activity, with results
29 summarized in Figure 12. Each model's decoding accuracies were subsequently
30 compared across various time bin durations and anatomical regions of the mouse visual
31 system. In our analysis, time bin durations of 50 ms and greater appeared to capture
32 neural information in the most robust way for decoding. Deep neural networks
33 outperformed shallow neural networks and linear support vector machines across nearly
34 all conditions (aside from small time bin durations, which was felt to be secondary to
35 overfitting) and within individual brain regions. VISp (primary visual cortex) outperformed
36 all other discrete brain regions in decoding accuracy, with VISal (anterolateral visual
37 cortex) and LGN (thalamic) closely behind, and CA1 and CA3 (hippocampal regions)
38 performing at chance, effectively serving as controls (Figure 12c). These findings suggest
39 possible avenues for future visual neural decoding efforts and offer insights into optimal
40 neural decoding algorithm design.
41
42
43
44
45
46
47
48
49
50
51
52
53
54
55
56
57
58
59
60

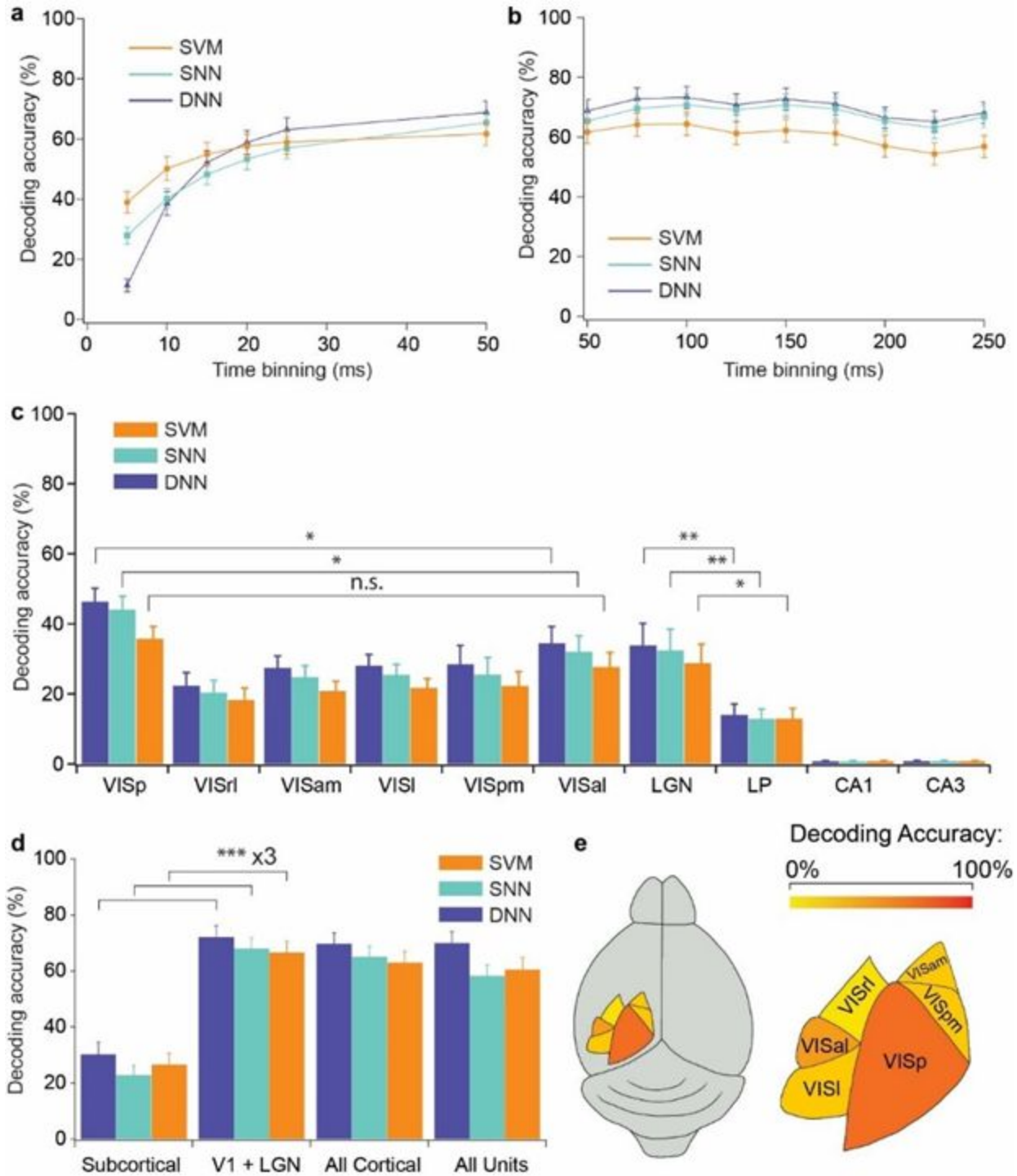


Figure 12. Neural Decoding Analysis. (a-b) Results of time binning analysis. Mean decoding accuracies of each time bin condition and machine learning model plotted and reported in the underlying table. (c) Individual brain region decoding analysis. Mean decoding accuracies across all sessions reported for each brain region and machine learning model, superimposed

1
2
3 on top of a table of values. (d) Grouped brain region decoding analysis. Graphical comparison
4 between mean decoding accuracies of various grouped brain regions for each machine learning
5 model, along with mean values. (e) Anatomical heatmap of decoding accuracies of six visual
6 cortex subregions decoded from, overlaid on mouse brain.
7
8
9

10 Several limitations exist, however. Data were obtained from an open dataset
11 provided by the Allen Institute, which may aid in reproducibility but inherently limited our
12 ability to acquire raw spiking data. Our deep learning and data analysis therefore relied
13 on data obtained by another institution. The interpretability of this work may be partially
14 limited given the unpredictable nature of the representations learned by deep neural
15 networks as evidenced by signs of overfitting described above. While our decoding
16 networks were validated, trained, and tested within each individual subject, it remains
17 unclear how well the models would generalize across subjects.
18
19
20
21
22
23
24

25 While conventional neural decoding algorithms make assumptions about the
26 encoding of neural representations, deep learning-based neural decoding makes few
27 assumptions. However, most deep learning-based neural decoding work has been done
28 in motor cortex decoding. Accurate decoding of electrophysiology signals from brain
29 structures involved in visual processing hold great promise in better informing our
30 understanding of sensory processing, artificial intelligence, and BCIs for visual
31 prosthetics. Taking a page from the motor decoding literature, future directions of this
32 work involve implementing a neural population dynamics approach given the richness of
33 spiking data in this open dataset. For example, characterizing the distinct neural
34 trajectories that visual scene stimuli produce, as has been described with movement
35 patterns in the motor cortex. Lastly, while our initial focus was decoding static visual
36 stimuli, reconstruction of both static and dynamic (movies) visual stimuli from action
37 potential spikes would represent a significant breakthrough, as has been explored in
38 recent years largely with fMRI.
39
40
41
42
43
44
45
46
47
48
49

50 **2.5.c. Presenter:** Mousa Mustafa (Technische Universität Berlin, Germany)
51

52 *Title:* Decoding Invasive Brain Signals Using Deep Learning
53
54

55 *Master:* Marianna Semprini, PhD (Italian Institute of Technology, Genoa, Italy)
56
57
58
59
60

1
2
3 *Theme:* Brain implant - other
4

5
6 This research explores the use of deep learning and classical machine learning
7 models to predict self-paced hand movements in patients with PD using ECoG
8 recordings. Deep learning has advanced the decoding of ECoG data [68], providing
9 insights into precise hand movements. Adaptive bidirectional neuromodulation, which
10 combines neurostimulation with real-time brain activity feedback, offers the potential for
11 more accurate symptom management for patients with PD [69]. Merk et al. [70] conducted
12 a comprehensive review on the current state of machine learning use for DBS, and these
13 developments underscore the promise of deep learning in neurology, including
14 applications in brain-computer interfaces and neuroprosthetics. The study's objective is
15 to compare the accuracy and precision of predictions made by these models and evaluate
16 their potential for use in closed-loop deep brain stimulation treatment for PD.
17
18
19
20
21
22
23
24

25 A variety of classical machine learning models (Logistic Regression, XGBoost
26 Classifiers, support vector machine, K-neighbor classifier, Random Forests, and Gradient
27 Boosting) and deep learning model architectures (CNN, ResNet, HTNet, and multilayer
28 perceptron) were used in this study. The models were trained on data recorded from
29 intracranial electrodes placed at the sensorimotor and parietal cortex of patients.
30 Preprocessing and frequency band variance features were extracted for the classical
31 machine learning models using the `py_neuromodulation` toolbox, while continuous
32 normalized ECoG data were used to train the deep learning architectures. After training
33 the models, validating them via 3-fold cross-validation, and evaluating them on the
34 balanced accuracy metric, it was observed that the best deep learning model
35 outperformed the classical machine learning models on most subjects in balanced
36 accuracy and in all subjects on the F1 score. A visualization of the processing pipeline
37 may be found in Figure 13a.
38
39
40
41
42
43
44
45
46
47

48 The results of this study demonstrate the potential of deep learning models in
49 accurately predicting self-paced hand movements using ECoG recordings from patients
50 with PD. The deep learning models outperformed the traditional machine learning models
51 in accuracy and precision. Specifically, the deep learning models achieved a balanced
52 accuracy with a mean of 0.8808 and a standard deviation of 0.0532, and an F1 score with
53
54
55
56
57
58
59
60

a mean of 0.7378 and a standard deviation of 0.0799. In comparison, the classical machine learning models had a balanced accuracy with a mean of 0.7875 and a standard deviation of 0.1071, and an F1 score with a mean of 0.5330 and a standard deviation of 0.1948 (Figure 13b). These findings suggest that deep learning models have the potential to be a valuable tool in the treatment of Parkinson's disease.

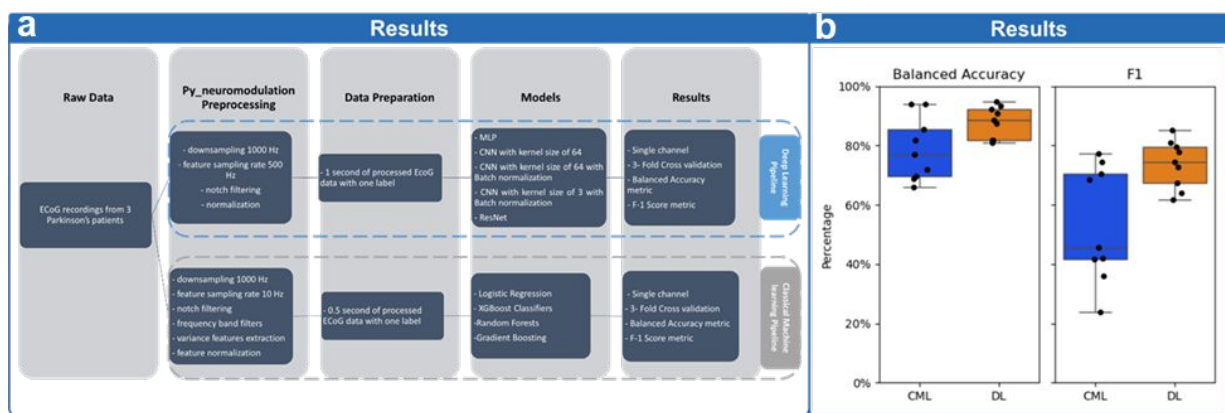


Figure 13. (a) Overview of the pipeline used for each model group. (b) comparison of the results on both the balanced accuracy score and F1 metrics between the classical machine learning (CML) group and deep learning (DL) group.

The study's limitations include a small sample size, data variability among patients and lack of model interpretability. Future research should focus on larger and more diverse cohorts, longitudinal studies, improving model interpretability, and exploring the effect of data size on training the deep learning models. Additionally, exploring real-world implementation in clinical settings is crucial. Addressing these aspects will help fully realize the potential of deep learning models in treating Parkinson's disease.

2.6 Exploring brain-computer interfaces for neurorehabilitation

For neurorehabilitation, BCIs serve as invaluable tools by translating neural signals into tangible feedback, thereby aiding patients in various situations, such as post-stroke rehabilitation or mental health improvement. By continually refining the design, enhancing feedback mechanisms, and broadening the clinical applications of BCIs in

1
2
3 neurorehabilitation settings, we can effectively customize these systems to meet the
4 unique needs and preferences of each user.
5

6
7 **2.6.a. Presenter:** Jose Gonzalez-Espana (University of Houston, USA)
8

9
10 Title: NeuroExo: A Low cost Non Invasive Brain Computer Interface for upper-limb
11 stroke neurorehabilitation at home
12

13
14 Master: Ning Jiang, PhD (University of Waterloo, Canada)
15

16 Theme: Brain non-implanted - control
17

18
19 EEG-based BCIs for real-time control of end effectors in at-home
20 neurorehabilitation demand robust software and hardware solutions. However, the high
21 cost of quality EEG amplifiers hinders their commercial viability. In the NeuroExo BCI
22 System, it addressed these challenges by developing a low-cost BCI system with a focus
23 on democratized access. Specifically designed for upper-limb stroke rehabilitation, the
24 NeuroExo BCI System serves as a groundbreaking proof of concept.
25
26

27
28 The system comprises key components, including a versatile EEG headset with
29 five dry-comb electrodes for a form-fitting, universally adaptable solution. Using cost-
30 effective devices such as the BeagleBone Black Wireless, ADS1299, and ICM-20948 for
31 processing and data collection, we ensured affordability. LabVIEW facilitated seamless
32 integration as the primary coding language. The NeuroExo BCI system has real-time
33 capabilities in both open and closed-loops modes. In open loop mode, raw EEG and
34 inertial measurement unit data were collected at an 80 Hz rate, while in the closed loop
35 mode, a WiFi-enabled robotic arm served as the end effector for upper-limb rehabilitation
36 at a 40 Hz rate.
37
38

39
40 To validate the system's clinical utility for at-home neurorehabilitation, stroke
41 survivors enrolled at TIRR Memorial Hermann participated in a comprehensive program.
42 This included one week of clinic training followed by six weeks of home therapy with the
43 NeuroExo BCI system, with progress assessed by a physical therapist before and after
44 sessions. The goal of the NeuroExo system is to enhance the feasibility of at-home
45 neurorehabilitation for chronic stroke patients, offering a low-cost, portable, reliable, and
46 user-friendly solution.
47
48
49
50
51
52
53
54
55
56
57
58
59
60

1
2
3 In future work, the results of at-home use by stroke survivors and healthy
4 participants will be presented. A user-centered analysis of the system will also be
5 included. Improvements in the hardware, firmware, and both the back-end and front-end
6 software are expected to be implemented based on the user-centered experience.
7
8
9

10
11 **2.6.b. Presenter:** Florencia Garro, PhD (Italian Institute of Technology, Genoa, Italy)

12
13 *Title:* Effects of Robotic Assistance in ERP Modulation for Upper-limb Exoskeleton
14 Control
15

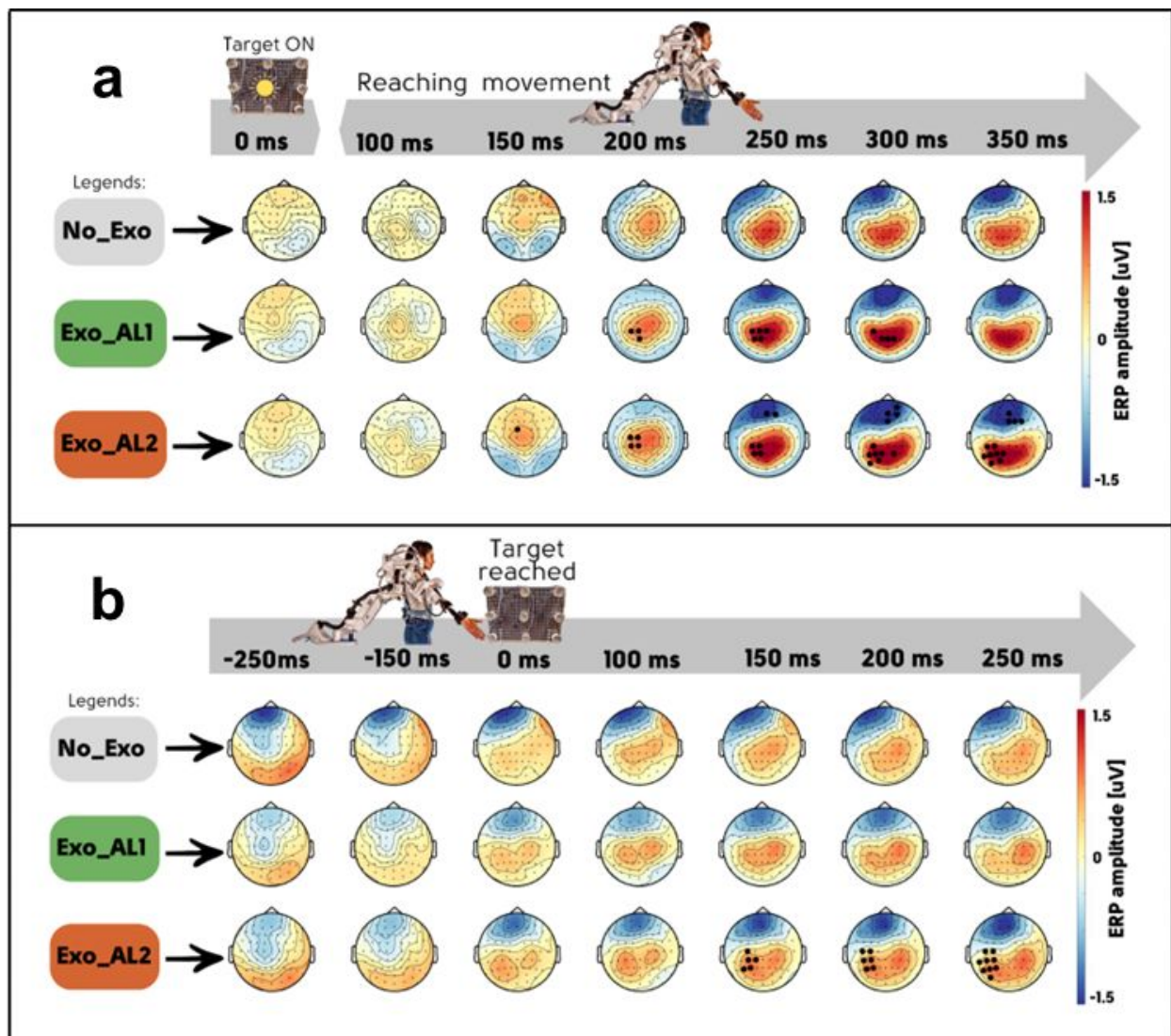
16
17 *Master:* Ning Jiang, PhD (University of Waterloo, Canada)
18

19
20 *Theme:* Brain non-implanted - control
21

22 Event-related potential (ERP)-based BCIs are investigated in robotic
23 neurorehabilitation to potentially boost brain plasticity and motor learning by engaging
24 patients in the control loop [71]. Exoskeletons offer assistance levels (ALs) that could be
25 fine-tuned using ERP-based BCI [72]. However, it remains unclear if and how brain
26 activity is affected by varying ALs. We analyze ERP modulation during a standardized
27 task with different ALs provided by FLOAT, a novel upper limb exoskeleton [73], to explore
28 the relationship between brain activity and ALs.
29
30
31
32
33
34

35 We collected high-density EEG from 10 healthy right-handed individuals while
36 performing a standardized reaching task under three distinct conditions: unassisted free
37 movement (No_Exo) and two levels of FLOAT-assisted movements: low and high AL
38 (Exo_AL1 and Exo_AL2). Between 100-350 ms after the Go cue, a cluster-based
39 permutation test using the Monte Carlo method shows differences in both **Exo_AL1** and
40 **Exo_AL2** vs **No_Exo** conditions ($p < 0.05$). The difference is most pronounced over
41 central, centroparietal, and left parietal-occipital sensors, including the frontocentral area
42 for **Exo_AL2** (Figure 14a). Between -250-250 ms centered on target reach, we found
43 differences between the **Exo_AL2** and **No_Exo** condition, most pronounced over central
44 and left parietal-occipital sensors (Fig. 14b). The lack of difference between Exo_AL1 and
45 No_Exo suggests that the motor scheme is unchanged, and thus, the two conditions are
46 perceived similarly in that movement phase.
47
48
49
50
51
52
53
54
55
56
57
58
59
60

1
2
3 Comprehending the impact of ALs on brain activity may boost BCI design, aiding
4 in the enhancement of human-in-the-loop optimization strategies for neurorehabilitation.
5 Specifically, future research aims to support the development of novel metrics based on
6 standardized neuromechanical data for assessing the performance of both robotics and
7 patients. Limitations of this study include the self-paced nature of the task, which may
8 introduce asynchrony in ERPs, and the small sample size. Future work will address these
9 limitations by expanding the sample size to enable more robust statistical analyses, and
10 by exploring additional analyses, such as frequency domain approaches.
11
12
13
14
15
16
17
18
19



1
2
3 **Figure 14.** ERP amplitudes for No_Exo (gray), Exo_AL1 (green), and Exo_AL2 (red) across
4 various time intervals centered on the Go cue (**a**) and target reach (**b**) conditions. Adapted from
5
6 [74] with permission.
7
8

9 **2.6.c. Presenter:** Angela Vujic, PhD (Massachusetts Institute of Technology, Boston,
10 USA)
11

12
13 *Title:* Joie: An Affective Brain-computer Interface for Learning Mental Strategies for
14 Positive Affect
15

16
17 *Master:* David E. Thompson, PhD (Kansas State University, USA)
18

19
20 *Theme:* BCI non-implanted - other
21

22
23 Training to enhance left prefrontal brain activity via neurofeedback may alleviate
24 symptoms of anxiety and depression [75,76]. To impart users with positive mental
25 strategies, we developed Joie, a joy-based EEG BCI [77,78]. Joie utilizes prefrontal alpha
26 asymmetries linked to joyful thoughts as input to control a character's movement in a
27 neurofeedback video game (Figure 15). The video game is designed as an endless
28 runner where users are rewarded and receive a score based on how long they sustained
29 left prefrontal asymmetry. Joyful thoughts during gameplay induce left prefrontal
30 asymmetry, resulting in positive feedback in-game, whereas right prefrontal asymmetry
31 results in negative feedback. In a lab study involving 20 participants undergoing 15
32 training sessions each over two weeks, our experimental group, instructed to imagine
33 positive music, winning awards, and other strategies associated with approach and
34 withdrawal motivation behavior, exhibited a significantly improved ability to activate alpha
35 asymmetry compared to placebo and control groups. Joie highlights the potential of
36 prefrontal asymmetries, or applying the approach and withdrawal motivation model, as
37 input for affective BCIs. Training these asymmetries via neurofeedback can impart mental
38 strategies with potential applications in mental health for reducing anxious or depressive
39 symptoms.
40
41
42
43
44
45
46
47
48
49
50
51
52
53
54
55
56
57
58
59
60

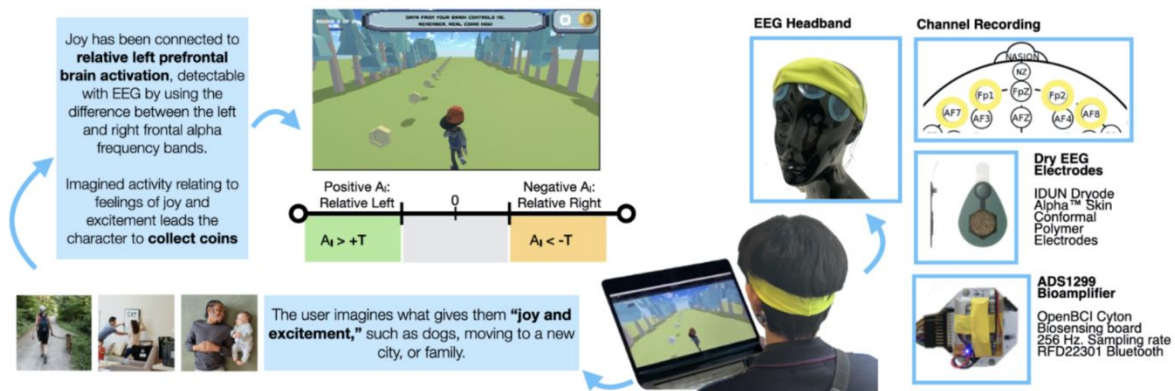


Figure 15. Joie's neurofeedback design with a wearable, dry electrode headband. The user imagines joyous thoughts activate prefrontal left asymmetries that cause their character to collect coins as a reward. Reprinted from [75] with permission.

2.7 Advancements in sampling the sensorimotor cortex

Recordings obtained from the sensorimotor cortex have played a pivotal role in advancing BCIs and their practical applications. Recent innovations in neural interface technology, such as endovascular electrode arrays, advancements in sampling techniques, such as ultra-high-density ECoG recordings, offer new avenues for capturing neural signals and extracting information. Despite these technological strides, there remains a crucial need to thoroughly characterize the information encoded within these novel signals and datasets to understand their applicability.

2.7.a. Presenter: Kriti Kacker (Carnegie Mellon University, USA)

Title: Spectral features of endovascular ECoG signals recorded from a Stentrode in human motor cortex

Master: Richard Andersen, PhD (California Institute of Technology, USA)

Theme: Brain implant - control

The Stentrode™ is a novel endovascular BCI technology implanted within the superior sagittal sinus to measure field potentials, similar to ECoG, from the primary motor cortex, enabling communication for individuals with severe paralysis [79]. However, the features of these vascular ECoG (VECoG) signals have not been fully characterized in

1
2
3 humans. Participants with severe paralysis due to amyotrophic lateral sclerosis and
4 brainstem stroke have been implanted in pilot clinical trials in Australia (n=4) and in an
5 Early Feasibility study in the United States (n=6).
6
7

8
9 We examined the VECoG signals from one US participant to identify spectral
10 features associated with volitional motor intent (Figure 16). The recorded field potentials
11 were filtered into standard frequency bands: alpha (8-13 Hz), beta (13-30 Hz), low gamma
12 (30-80 Hz), and high gamma (80-200 Hz). For each band-limited signal, we calculated
13 the change in root-mean-square voltage (V_{rms}) between rest and movement epochs,
14 quantifying the percentage change of V_{rms} movement from rest (termed as modulation
15 depth) for each trial.
16
17
18
19
20
21

22 We investigated the features of the Stentrode signals and identified the spectral
23 characteristics that exhibited strong and consistent changes in amplitude between rest
24 and attempted movement conditions. The average modulation depth across all channels
25 was $22.77 \pm 6.34\%$ in the low gamma band and $40.20 \pm 6.00\%$ in the high gamma band
26 during right hand movement. The classifier performance for both the gamma bands
27 remained stable, with the low gamma classifier achieving a mean accuracy of $93 \pm 3\%$
28 and the high gamma classifier achieving a mean accuracy of $96 \pm 3\%$. These results
29 suggest that the Stentrode reliably detects volitional motor signals and maintains long-
30 term stability for up to 10 months post-implantation. Our preliminary analysis indicates
31 that these endovascular neural signals exhibit properties similar to those reported for
32 ECoG-based measures of motor intent. Future research should explore VECoG signals
33 over a longer time period and across more participants to confirm that the BCI can operate
34 reliably and effectively over the course of several years.
35
36
37
38
39
40
41
42
43
44
45
46
47
48
49
50
51
52
53
54
55
56
57
58
59
60

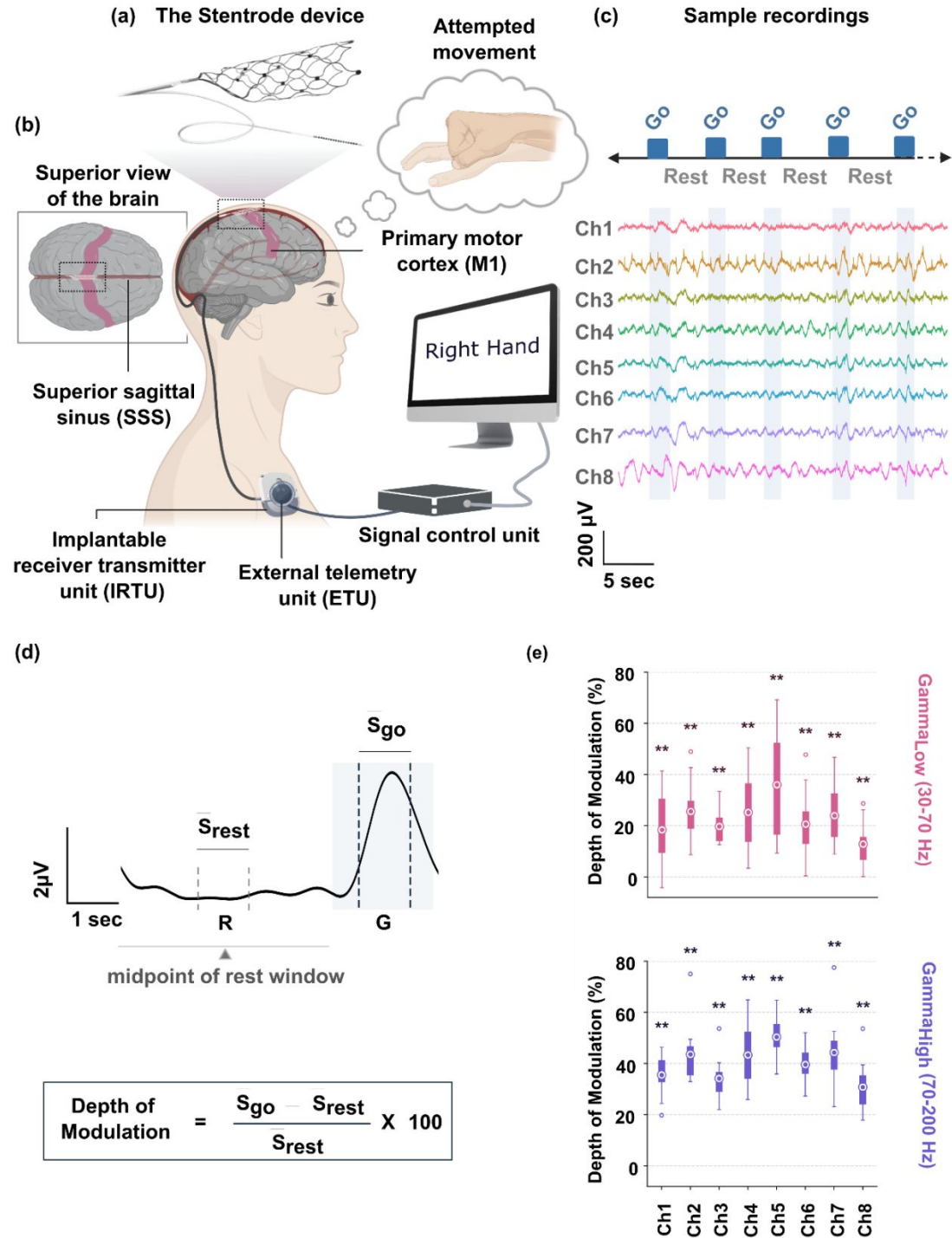


Figure 16. (a) The Stentrode device with 16 electrodes. (b) The Stentrode is a flexible electrode array implanted in the superior sagittal sinus using stent technology and sits adjacent to the primary motor cortex. The participants are instructed to attempt movement of specific body segments based on the cues on the screen. The data recorded by the Stentrode is sent

1
2
3 wirelessly to the external telemetry unit by the implantable receiver transmitted unit. The signal
4 control unit sends the data further to the computer. (c) Sample VECoG recorded from eight
5 channels during alternating cues of rest and go. (d) Modulation depth is calculated as the
6 percentage change in the average amplitude during attempted movement window (Sgo) with
7 respect to the average amplitude during the rest window (Srest). (e) Modulation depth for
8 VECoG signals across all channels in the low gamma and high gamma bands while the
9 participant attempted to move their right hand. ** Indicates t-test was significant at $p < 0.01$.

14
15 **2.7.b. Presenter:** Christoph Kapeller, PhD (g.tec medical engineering GmbH, Austria)

16
17 *Title:* Increased spatial resolution reveals separated EEG activation of individual finger
18 movements

19
20
21 *Master:* Christian Herff, PhD (Maastricht University, Netherlands)

22
23
24 *Theme:* Signal acquisition

25
26 The study of high-density EEG electrodes is currently of great interest in BCI
27 research. The 10-20 system, proposed by Jasper in 1958 [80], and the 10-10 extension
28 by Chatrian et al. in 1985 [81], are the established standards by the American EEG
29 society. In 2001, Oostenveld introduced the 5% system positions [82]. Our proposed
30 setup with active ultra-high-density electrode (uHD) records EEG via scalp grids with an
31 electrode spacing of 8.6mm, compared to a median Euclidean distance of 35.4mm in the
32 10-10 system (Figure 17). This represents a four times higher spatial sampling, combined
33 with an increased R^2 of the cross-channel EEG from 0.18 to 0.44, indicating a net increase
34 of information content over all EEG signals [83]. Studies have shown that biomarkers for
35 individual finger extensions achieved classification accuracy for two fingers by +6-7%
36 from 10-10 EEG to uHD EEG [84,85]. Specifically, with a grand average accuracy of
37 64.8% and a maximum of 79.2% for index versus ring finger [83]. A within-subject analysis
38 of the uHD EEG vs 10-10 EEG showed a clear reduction of channels with multi-finger
39 activation with more focused single finger sites over the motor cortex. Moreover, it is
40 possible to discriminate between hand gestures and their imagination, namely, rock-
41 paper-scissors, with 72.7% and 71.3%, respectively, in a pair-wise classification [86],
42 demonstrating the utility of a uHD EEG.

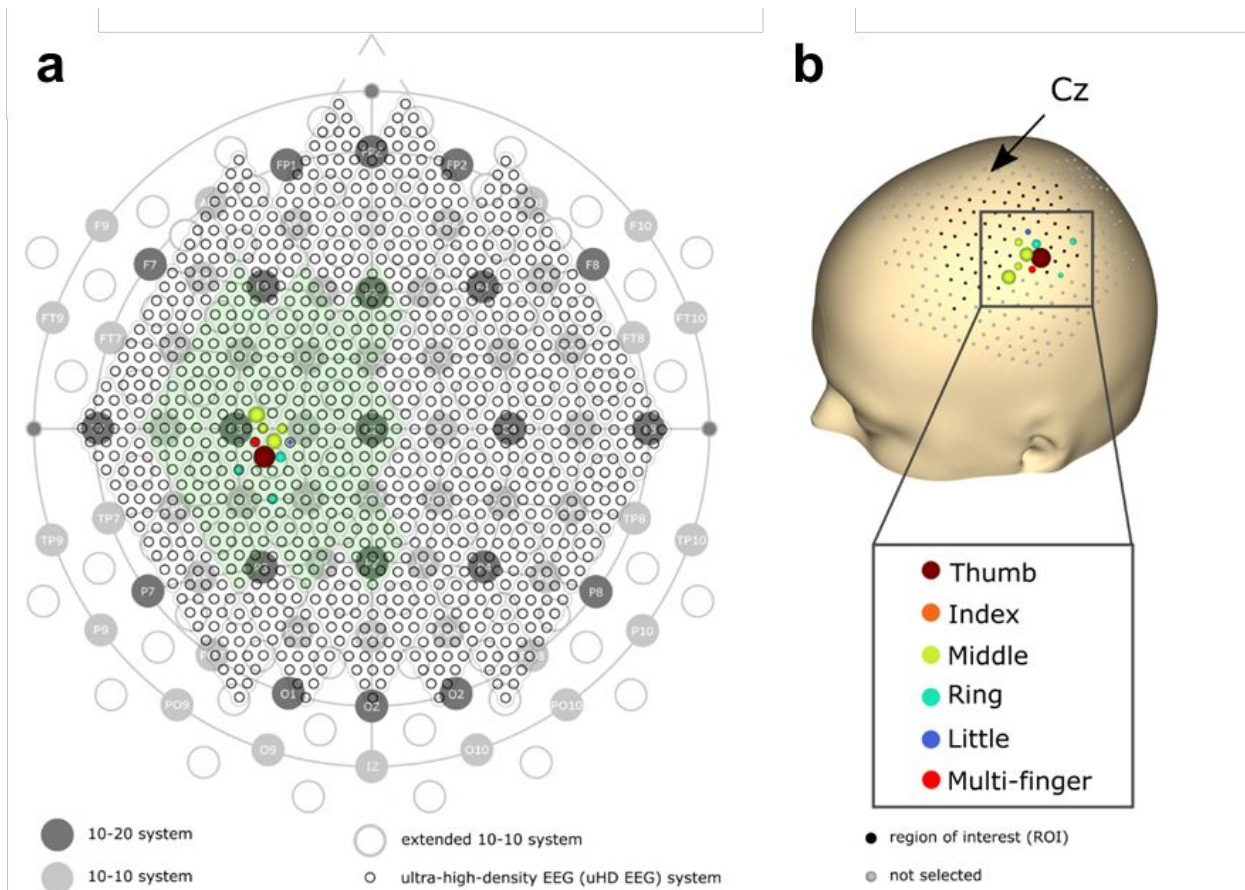
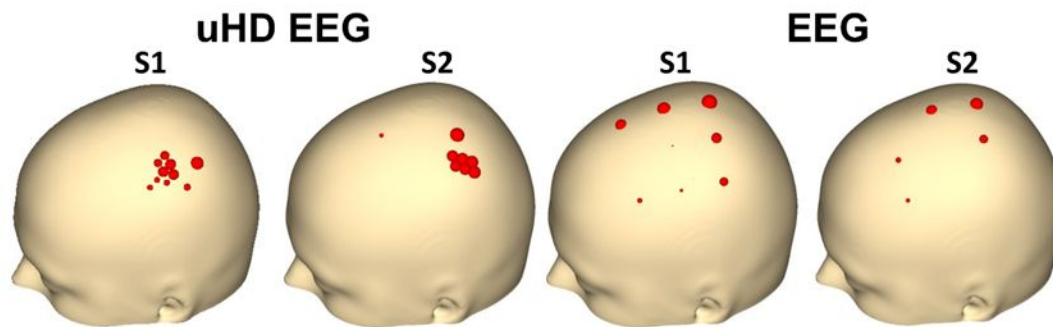


Figure 17. A focal point overlying the sensorimotor cortex around the 10-20 position C3 shows the highest activation. Ten electrodes were color-coded according to the finger with the greatest significance in ERD/S change, one finger includes information from several fingers (Multi-finger).

A subject specific example is provided in Figure 18, which represents the superimposed finger activity from Subject 1 on the electrode distribution comparison plot (a) and the MNI head (b). Results show the analysis of the beta band (13-30 Hz), which was used for feature extraction. After calculating the Event-related synchronization/desynchronization (ERD/S), a Wilcoxon signed-rank test was used to find significant channels with movement-related beta band changes. Significant channels are colored respectively for each finger and multi-finger channels, which were found to be active for several individual fingers. Figure 2 shows that ultra-high density / 10-10 beta power revealed 11% / 11% single-finger, 1% / 61% multi-finger and 88% / 28% no-finger sites, respectively. ERD/S bubble plots reflect the radius from the active channels' ERD/S amplitude.



Subject	S1 (uHD EEG)	S2 (uHD EEG)	Merged (uHD EEG)	S1 (EEG)	S2 (EEG)	Merged (EEG)
ROI (channels)	73	73	146	9	9	18
Significant channels	10	8	18	8	5	13
Single-finger	12%	10%	11%	11%	11%	11%
Multi-finger	1%	1%	1%	78%	44%	61%
no-finger	86%	89%	88%	11%	44%	28%

Figure 18. Significant channels marked in red from the single finger movement paradigm comparing the uHD EEG and 10-10 EEG system. The bubble radius reflects the ERD/S amplitude. The table states the region of interest selected, the number of significant channels and the ratio of single and multi-finger activation.

As our study included only two subjects, the results are not generalizable. A larger cohort, encompassing both male and female participants, as well as varying preferred hand dominance, is necessary to improve the robustness and applicability of the findings. For optimal system performance of the ultra-high-density EEG system, hair removal is essential, as effectiveness diminishes with increased hair length. Comprehensive testing across various hair types is necessary to identify potential limitations. Additionally, as the number of electrode grids increases, the system's form factor becomes more complex, leading to extended setup times and reduced user comfort. Future research should integrate uHD EEG with source reconstruction techniques to further refine high-resolution neurophysiological localization through non-invasive recordings.

1
2
3 **2.7.c. Presenter:** Simon Geukes (UMC Utrecht Brain Center, Netherlands)
4

5 *Title:* Ultra-high-density electrocorticography recordings of the human sensorimotor
6 cortex
7

8
9 *Master:* Victoria Peterson, PhD (Instituto de Matemática Aplicada del Litoral, Santa Fe,
10 Argentina)
11

12
13 *Theme:* Signal analysis
14
15

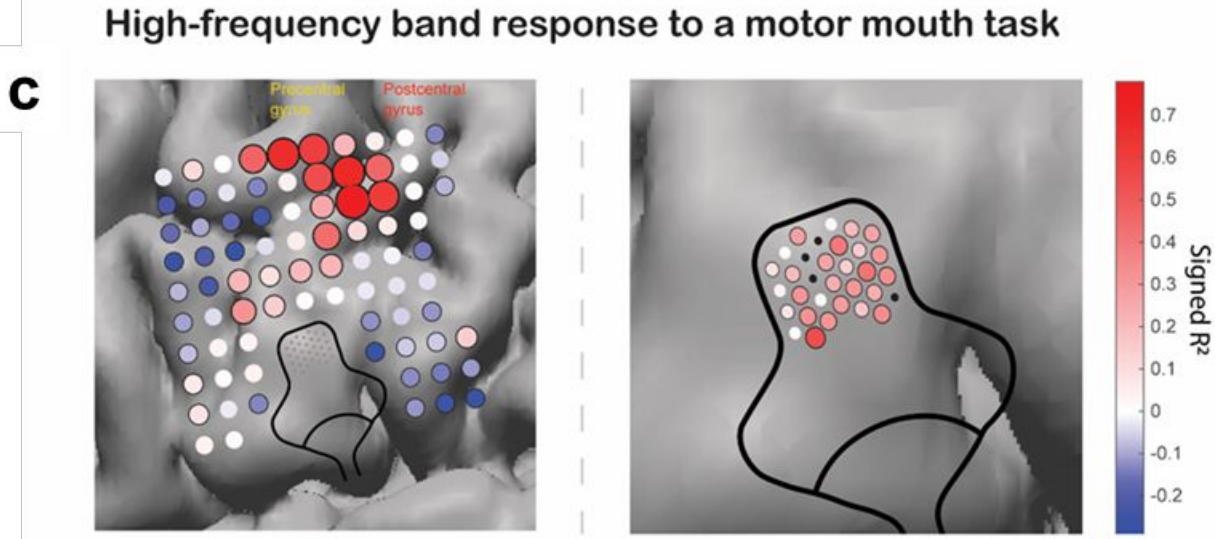
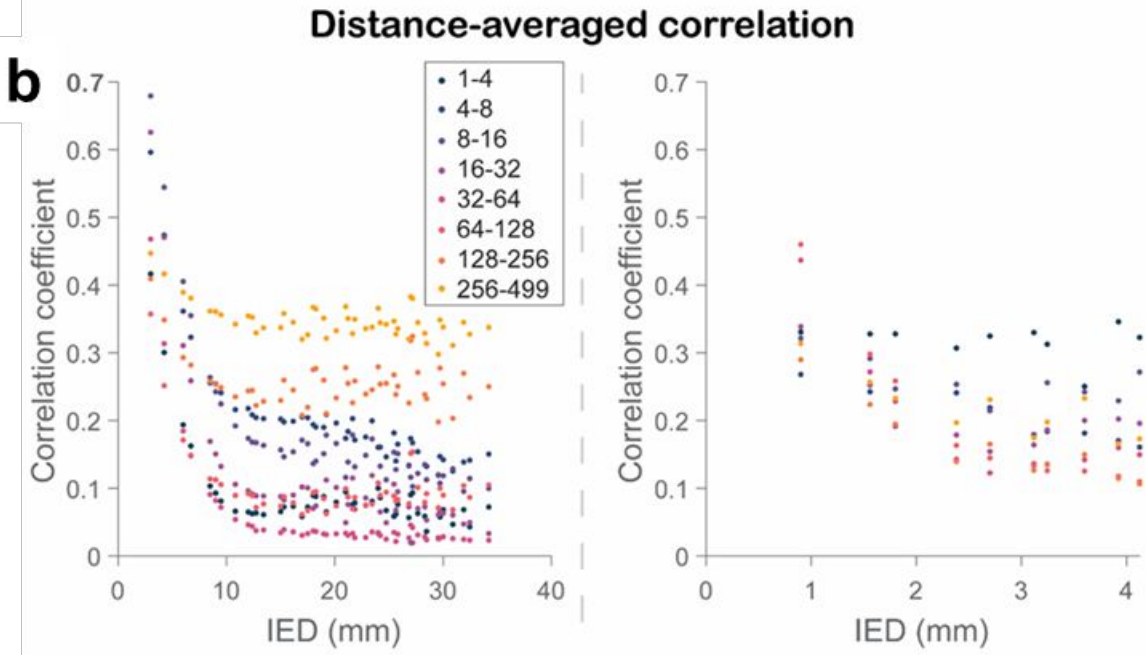
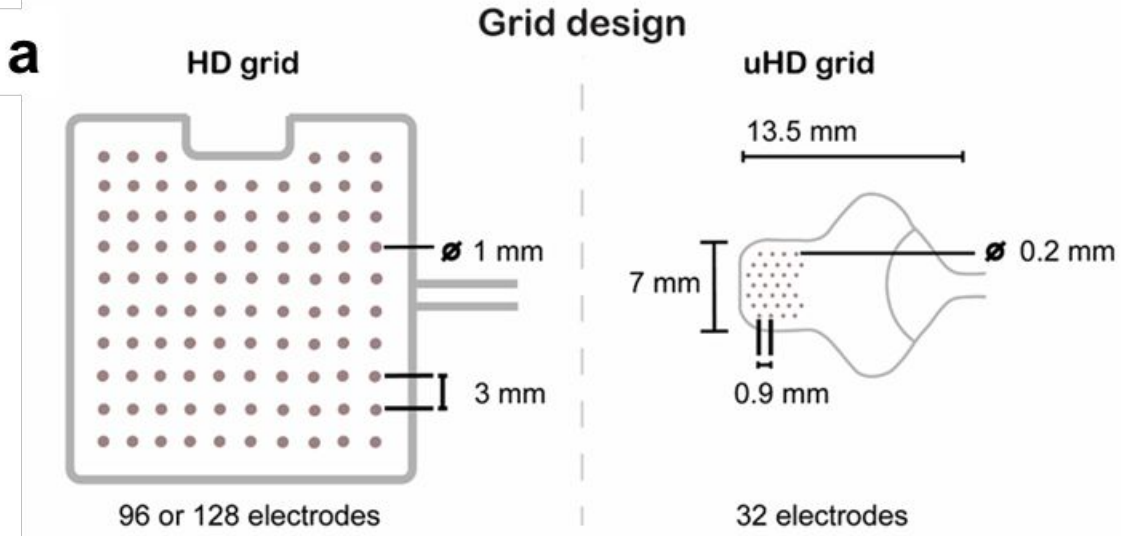
16 ECoG is a popular recording method for clinical and research purposes, including
17 brain-computer interfaces [87]. Clinical ECoG grids have 10 mm inter-electrode distance
18 (IED), while high-density (HD) ECoG grids have 3-4 mm IED. Both clinical and HD ECoG
19 may spatially undersample the cortex, as the cortical resolution is higher than the
20 resolution offered by these grids [88,89]. Ultra-high-density (uHD) ECoG, which offers
21 submillimeter resolution, may resolve this. However, whether uHD ECoG can record
22 distinct neural signals without considerable spatial oversampling remains unclear.
23
24
25
26
27
28

29 To investigate this, we simultaneously recorded intraoperative HD and uHD ECoG
30 (Figure 19a-b) from the sensorimotor cortex while participants were awake (n=3) or under
31 general anesthesia (n=1). During awake surgeries, the participants performed motor
32 mouth or hand tasks. To verify signal quality, we computed the power spectra of the
33 recorded signals. To investigate overlap between electrodes as a function of IED, we
34 calculated the distance-averaged correlation: the average correlation coefficient between
35 equidistant electrode pairs, for different frequency bands. Lastly, to quantify functional
36 responses, we regressed the mean high-frequency band power (64-128 Hz) to the tasks.
37
38
39
40
41
42

43 We found that: 1) In all participants, the 1/f decay and noise peaks were similar in
44 the power spectra of HD and uHD grids; 2) In three participants, HFB power overlapped
45 only moderately (r : 0.35-0.65) between electrodes at 0.9 mm IED. This is illustrated in
46 Figure 19c, which shows the distance-averaged correlation for the HD and uHD grid of
47 one participant. 3) In one participant, 70% of the uHD electrodes significantly responded
48 to the task, revealing a distinct spatial pattern where certain electrodes responded
49 significantly while adjacent ones did not. Taken together, we conclude that uHD ECoG
50 does not spatially oversample the sensorimotor cortex. Further investigation into optimal
51
52
53
54
55
56
57
58
59
60

1
2
3
4
5
6
7
8
9
10
11
12
13
14
15
16
17
18
19
20
21
22
23
24
25
26
27
28
29
30
31
32
33
34
35
36
37
38
39
40
41
42
43
44
45
46
47
48
49
50
51
52
53
54
55
56
57
58
59
60

recording procedures, re-referencing methods and analytical methods to quantify single electrode responses are needed to fully leverage the potential of uHD ECoG.



1
2
3 **Figure 19.** (a) Left panel: illustration of the 96-channel HD grid (Ad-Tech Medical, Oak Creek,
4 USA). A 128-channel grid (PMT Corporation, Chanhassen, USA) with the same IED and
5 exposed diameter was used as well. Right panel: illustration of the uHD grid (CorTec Neuro,
6 Freiburg, Germany). (b) Distance-averaged correlation for the HD grid (left panel) and uHD grid
7 (right panel) of one participant. The frequency bands (in Hz) are denoted by the color coding. (c)
8 High-frequency band response (64-128 Hz) to a motor mouth task for the HD grid (left panel)
9 and uHD grid (right panel) of one participant. HD electrodes overlaying the uHD grid are not
10 shown. Excluded electrodes are colored black. Electrode radius increases with the R2 value.
11 Circumvented electrodes responded significantly to the task. (a) and (c) are adapted, with
12 permission, from[90].
13
14
15
16
17
18
19

20 **2.8 Novel techniques for advancing brain-computer interface performance**

21
22 Integrating multiple modalities, such as incorporating both brain signals and other
23 physiological signals as input, merging brain recordings with stimulation techniques, or
24 exploring new analytic techniques hold promise for advancing BCI control and decoding
25 capabilities. By harnessing the complementary strengths of diverse signals, BCI systems
26 stand to benefit from heightened efficacy and enhanced accuracy, thereby amplifying
27 their use in real-world applications. Moreover, developing innovative strategies for
28 encoding movement patterns, optimizing dynamic stopping methods for diverse
29 applications, and augmenting motor skill acquisition may unlock new dimensions of BCI
30 functionality.
31
32
33
34
35
36
37

38 **2.8.a. Presenter:** Tan Gemicioglu (Cornell University, USA)

39 *Title:* Transitional Gestures for Enhancing ITR and Accuracy in Movement-based BCIs

40
41
42
43 *Master:* Ning Jiang, PhD (University of Waterloo, Canada)

44
45
46 *Theme:* BCI non-implanted - control
47

48 Motor imagery and motor attempt-based BCIs enable users to communicate by
49 sequentially performing different actions. Conventional interaction methods use a set of
50 body parts or motions with a one-to-one mapping to commands. However, this mapping
51 makes it challenging to use movement for high-speed spellers due to constraints in the
52 number of possible commands. A recent interaction method, BrainBraille, uses a pseudo-
53
54
55
56
57
58
59
60

1
2
3 binary encoding where up to six body parts can be tensed simultaneously and mapped
4 onto a Braille character for language-independent alphabetic encoding. However, non-
5 invasive BCI modalities such as EEG and functional-near infrared spectroscopy (fNIRS)
6 have limited spatial specificity and often struggle to distinguish simultaneous movements.
7
8

9
10 We propose a new method encoding transitions between gestures in different body
11 parts to combinatorially increase the size of the command set by using transitional
12 gestures where information is extracted from transitions between different movements to
13 improve accuracy, number of possible commands, and information transfer rate (ITR). In
14 a pilot study using the NIRx NIRSport, participants tensed the left hand and right hand in
15 transitional patterns in a random order for 40 trials each. We applied a 0.09Hz low-pass
16 Butterworth filter and performed independent component analysis. A support vector
17 machine obtained 81% accuracy in left vs. right classification while obtaining 92%
18 accuracy in left-to-right vs right-to-left classification, demonstrating the accuracy benefits
19 of transitional gestures.
20
21

22
23 Then, we adapted the BrainBraille encoding scheme with a transitional encoding.
24 BrainBraille is currently limited to a maximum of three simultaneous movements and uses
25 27 out of 37 possible commands. Our transitional BrainBraille encoding would allow
26 $P(6,3)=120$ commands, allowing a wider range of characters while maintaining the same
27 constraints and potentially increasing ITR from BrainBraille's current ITR of 143 bits per
28 minute to 218 bits per minute. Our findings suggest that a transitional encoding can make
29 a movement-based speller more feasible by increasing accuracy, speed, and flexibility in
30 modalities with limited spatial specificity.
31
32

33
34 **2.8.b. Presenter:** Ceci Verbaarschot, PhD (University of Pittsburgh, USA)
35

36
37 *Title:* The effect of artificially created sensory feedback on motor cortex activity during
38 task performance
39

40
41 *Master:* Marianna Semprini, PhD (Italian Institute of Technology, Genoa, Italy)
42

43
44 *Theme:* BCI implant - other
45
46

47
48 Intracortical microstimulation (ICMS) of the human somatosensory cortex induces
49 localized sensations on an individual's paralyzed hand and can enhance control of a
50
51
52
53
54
55
56
57
58
59
60

1
2
3 brain-controlled prosthetic arm [91,92]. Typically, there exists a direct interaction between
4 naturally occurring tactile sensations and motor function. Ongoing sensory input
5 influences the activity of the motor cortex, leading to intricate patterns of both inhibitory
6 and excitatory responses. We investigated whether artificial touch (created via ICMS)
7 could have a similar effect on motor cortex activity.
8
9

10
11
12 Two participants with tetraplegia with implanted intracortical microelectrode arrays
13 in their somatosensory and motor cortices (Figure 20a) underwent ICMS trains of various
14 amplitudes (40, 60, 80 μ A) and frequencies (50, 100, 200 Hz), while they passively
15 watched a movie. Next, we investigated the effect of ICMS (50 Hz, 60 μ A) while they
16 attempted (full hand grasp or individual finger) movements during an engaging Guitar
17 Hero-like game (Figure 20b). We found that higher stimulation amplitudes linearly
18 increased the global population activity in the motor cortex (Figure 20c). Meanwhile,
19 frequency had varying effects in which stimulation at 50 Hz had a largely excitatory effect,
20 200 Hz had a predominantly inhibitory effect, and lastly 100 Hz had mixed effects
21 depending on the electrode (Figure 20c). Despite prominent effects on motor cortex
22 activity, offline decoding of three individual fingers showed promise (89% accuracy)
23 during 50 Hz ICMS.
24
25
26
27
28
29
30
31
32
33

34 Our findings suggest that ICMS not only creates an artificial sense of touch during
35 motor control but also modulates motor cortex activity in a stimulus-dependent manner.
36 Under normal circumstances, dynamically evolving sensory input likely modulates motor
37 cortex activity, enabling us to, e.g., tighten our grip when we sense that an object is
38 slipping from our hands. In future research, we investigate whether ICMS could play a
39 similar functional role during motor control. To do so, we will manipulate the congruency
40 of the ICMS-evoked sensation location and the ongoing motor task. Often, participants
41 will feel a sensation on the same finger that they attempt to move during the Guitar-Hero
42 like game. Occasionally, we will evoke a sensation on a different finger, one that is
43 incongruent with the ongoing motor task. If we find the motor cortex to encode the
44 congruency of the sensory signal with the motor task, this will provide credence that ICMS
45 can serve as a functional source of information during motor control.
46
47
48
49
50
51
52
53
54
55
56
57
58
59
60

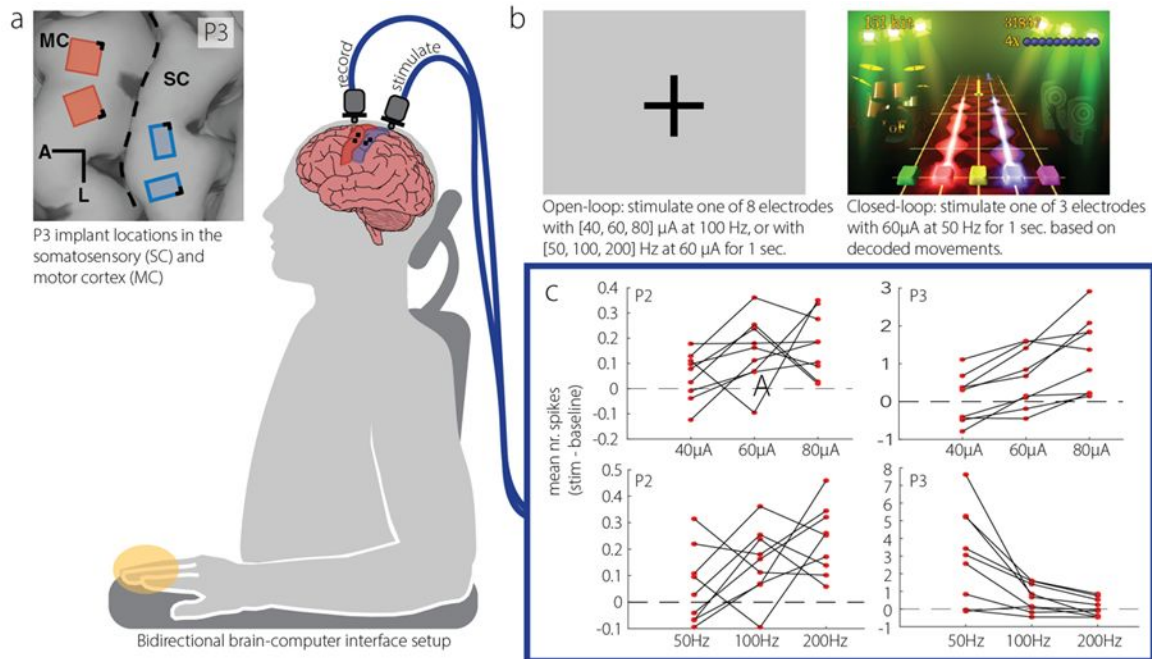


Figure 20. Overview of study design and results. (a) Schematic illustration of the BCI setup. (b) Experimental design using either open-loop (left) or closed-loop (right) stimulation. (c) Main results of intracortical microstimulation in the somatosensory cortex on the motor cortex for different amplitudes (top) and frequencies (bottom).

2.8.c. Presenter: Michael Wimmer (Know Center Research GmbH, Austria)

Title: Toward Hybrid BCI: EEG and Pupillometric Signatures of Error Perception in an Immersive Navigation Task in VR

Master: Marianna Semprini, PhD (Italian Institute of Technology, Genoa, Italy)

Theme: BCI non-implanted - other

The latest wearable devices used to visualize virtual reality (VR) content are equipped with built-in sensors and cameras to acquire user-specific physiological data, such as gaze or pupil size. Interactions with virtual environments may sometimes seem erroneous to users, as the behavior of the VR might not align with the user's intentions or expectations. Previous research has shown that EEG responses to errors, i.e., error-related potentials (ErrPs), can enhance the performance of BCIs [93]. The successful decoding of errors allows systems to take corrective actions, e.g., to stop unwanted

1
2
3 commands or provide visual aids. Since most error classifiers rely on brain signals, this
4 study explores the potential of pupillometric signals for hybrid error decoding approaches.
5
6

7 For this purpose, we designed an interactive VR flight simulation in which 19
8 participants navigated a glider through a series of targets (Figure 21). At random intervals,
9 participants encountered unexpected behaviors or changes in the simulation, such as
10 sudden displacements of the target locations and unintended glider movements.
11
12
13

14 The grand average responses revealed pupil dilations peaking approximately 600
15 ms after the error events. ErrPs were consistent with the existing literature [94]. The pupil
16 dilations exhibited considerable variability across participants, which affects the
17 performance and generalizability of classifiers. However, hybrid decoding approaches
18 could significantly improve the accuracy in reduced EEG setups, i.e., using only one or
19 three electrodes, by up to 3 to 4% on average and up to 8% at the participant level [95].
20 Studying the impact of such setup reductions has practical relevance, as they increase
21 the BCI's usability in real-world applications. Further analysis of the behavioral data
22 showed that participants took on average more than 400 ms to react to error events. The
23 offline error decoders we implemented could detect errors up to 50 ms faster than
24 participants responded to them [96].
25
26
27
28
29
30
31
32
33

34 The results of this work suggest that error-related pupillometric responses have
35 the potential to improve existing error decoding approaches and hence, the design of
36 hybrid BCIs [95]. Next steps in advancing hybrid classifiers should include research on
37 suitable features derived from pupil signals. Similarly, investigations into the impact of
38 different data fusion approaches could further enhance the decoding performance.
39 Finally, these contributions should be tested in real-time scenarios where the VR adapts
40 dynamically to errors.
41
42
43
44
45
46
47
48
49
50
51
52
53
54
55
56
57
58
59
60

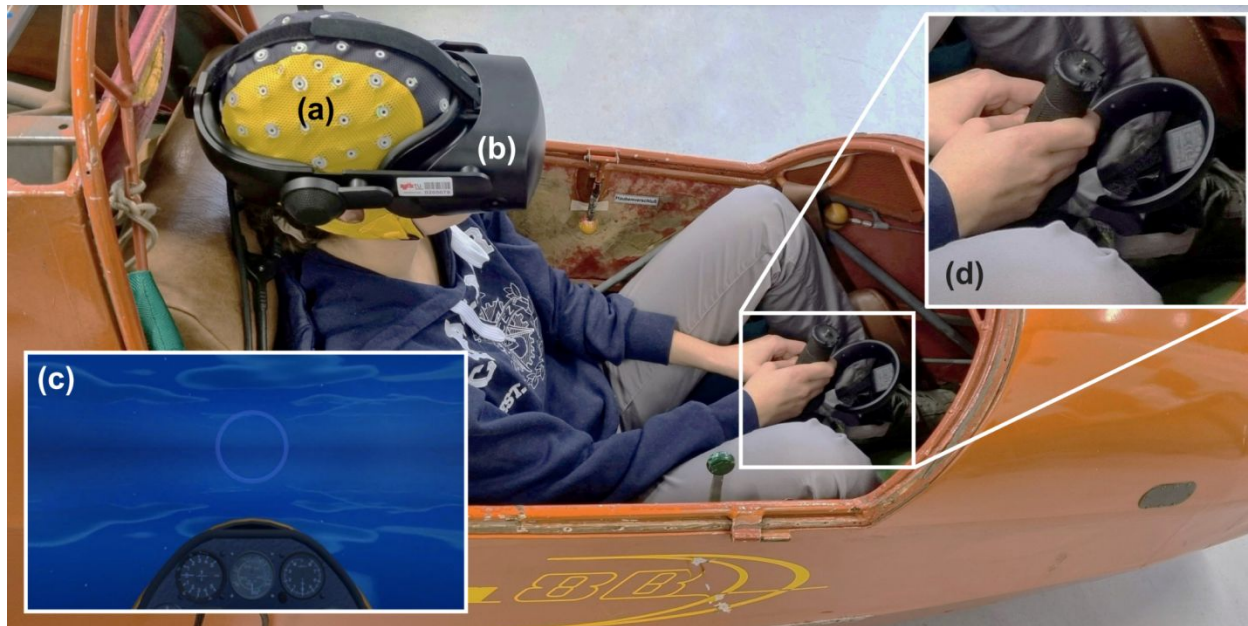


Figure 21. Overview of the experimental setup. The participant is seated in a glider, wearing an EEG cap (a) and an HMD (b) to interact with the virtual environment (c). The joystick of the HMD (d), used to navigate the virtual glider, is attached to the physical glider's control stick.

Figure adapted from [95] with author consent.

2.8.d. Presenter: Mushfika Sultana (University of Essex, United Kingdom)

Title: Assessing the impact of transcranial Direct Current Stimulation on the enhancement of race driving skills

Master: Eli Kinney-Lang, PhD (University of Calgary, Canada)

Theme: BCI non-implanted - other

Recently, non-invasive brain stimulation like transcranial direct current stimulation (tDCS) has become popular and has been applied to focally change neuronal activation [97]. Although tDCS seems to be a promising approach for enhancing complex motor skill acquisition, very few studies have investigated the potential role of brain stimulation on race driving [98]. We have attempted an initial evaluation of the impact of anodal tDCS on race training. Toward this goal, we have analyzed multimodal experimental data consisting of EEG and telemetry from a driving simulator of 11 novice participants.

1
2
3
4
5
6
7
8
9
10
11
12
13
14
15
16
17
18
19
20
21
22
23
24
25
26
27
28
29
30
31
32
33
34
35
36
37
38
39
40
41
42
43
44
45
46
47
48
49
50
51
52
53
54
55
56
57
58
59
60

Twenty minutes of active or sham tDCS (PlatoWork by PlatoScience, Copenhagen, Denmark) was applied before a race driving task. Subjects were randomly and blindly assigned to one of two tDCS groups (6 active, 5 sham) balancing potential confounding factors (age, gender, driving proficiency, corrected vision). Each participant went through 10 experimental sessions (20 laps per session). The tDCS effect was evaluated through a mixed-design ANOVA where the lap time gain as a result of training was the response variable, the tDCS group was the between-subjects factor and the session index was the within-subjects factor. Furthermore, we assessed the average, standard deviation, and significance (with unpaired, two-sided Wilcoxon rank sum tests) of the lap times per group and session. Although no significant effect of tDCS on lap time gain can be established ($F=0.63$, $p=0.76$), additional post-hoc analysis showed that subjects in the active tDCS group exhibited better outcomes in sessions where intense learning takes place. Specifically, active-tDCS subjects performed in the last session significantly better (by almost 3 s on average) than sham-tDCS (active: 89.4 ± 9.5 , sham: 92.0 ± 10.5 , $p<10^{-17}$), although performance was balanced (no statistically significant difference between the two groups) in the first session.

These preliminary results suggest that tDCS may be effective in supporting the learning of race driving, although the impact is not strong enough to be clearly observed in a session-wise, mixed-design ANOVA. It is important to note that the small sample size may account for the absence of a pronounced effect. Our findings indicate that tDCS can help novice users learn race driving more quickly, but the effect was modest and requires confirmation in future research. Further studies with larger populations will seek to clarify and validate these results.

2.8.e. Presenter: Sara Ahmadi, PhD (Radboud University, Netherlands)

Title: A model-based dynamic stopping method for code-modulated visual evoked potentials BCI

Master: Xing Chen, PhD (University of Pittsburgh, USA)

Theme: Signal analysis

1
2
3 BCI are evolving beyond mere assistive technology, with dynamic stopping
4 methods offering a means to expedite their speed [99]. These methods allow for decisions
5 to be made regarding symbol ejection or further information acquisition based on the
6 decoder's confidence level, thereby leveraging trial variance to enhance speed without
7 compromising overall accuracy. However, conventional optimization metrics like symbols
8 per minute and ITR may not adequately reflect system performance for specific
9 applications or user types.

10
11
12 In our proposal, we advocate for a model-based approach harnessing analytical
13 insights into the underlying classifier model. By establishing that similarity scores between
14 observed and predicted responses for both target and non-target classes follow Gaussian
15 distributions, we frame the dynamic stopping as a binary hypothesis decision problem.
16 Here, different costs are assigned to various courses of action, with the cost ratio (CR)
17 representing the ratio between the cost of False Alarm and Miss. Using a likelihood ratio
18 test based on Bayes criterion, we determine the decision region where the total risk,
19 calculated as the sum of costs weighted by the likelihood of each action, is minimized
20 [100].

21
22 Preliminary findings on a code-modulated visual evoked potential dataset [101]
23 demonstrate the efficacy of our approach. By adjusting the cost ratio, we observed
24 varying trade-offs between speed and accuracy. For instance, with a small cost ratio, the
25 system exhibits rapid response times (average time = $318ms$ for $CR=1$) but relatively high
26 error rates ($Err=81.9\%$ for a 36-class problem), which may suit applications where post-
27 processing, such as employing a language model, can compensate for lower accuracy.
28 Conversely, increasing the cost ratio to $CR=10^6$ extends response time (average time =
29 2.32 seconds) while substantially reducing error rates ($Err=22.9\%$), rendering the system
30 more suitable for error-sensitive applications.

3. Conclusions

31
32
33 The Tenth International BCI Meeting provided a platform for trainees to showcase
34 their research and engage in meaningful discussion with experts and the BCI community
35 through master classes. The sessions, organized by the Postdoc & Student Committee
36
37
38
39
40
41
42
43
44
45
46
47
48
49
50
51
52
53
54
55
56
57
58
59
60

1
2
3 of the BCI Society, were designed to foster interactions between trainees and established
4 researchers and encourage a conducive environment for learning and collaboration. The
5 master classes are a unique way to showcase the breadth of BCI research, illuminating
6 both the challenges and breakthroughs encountered across various fields.
7
8
9

10
11 The selected summaries featured in this paper offer insights into the multifaceted
12 topics explored in BCI research, reflecting the ongoing efforts of researchers to advance
13 technology. Divided into eight specific themes, including speech decoding, motor
14 imagery, and closed-loop BCIs, each summary presents the presenter's work, preliminary
15 findings, and conclusions. Notably, the inclusion of trainees and senior researchers as
16 co-authors emphasizes collaboration and mentorship within the BCI community. The
17 master classes will continue to highlight the remarkable contributions of BCI trainees at
18 the upcoming Eleventh International BCI Meeting.
19
20
21
22
23
24

25 **Acknowledgements**

26
27 The authors thank the National Institute on Deafness and other Communication Disorders
28 (NIDCD), the National Institute of Neurological Disorders and Stroke (NINDS), and the
29 National Science Foundation for sponsoring 2023 Trainee Awards to the Tenth
30 International BCI Meeting.
31
32
33
34

35 **Abbreviations**

36
37 aDBS - adaptive deep brain stimulation
38

39
40 AL - assistance level
41

42
43 ANN - artificial neural network
44

45
46 BRAND - Backend for Realtime Asynchronous Neural Decoding
47

48
49 BCI - brain-computer interface
50

51
52 BOTDA - backward formulation of optimal transport for domain adaptation
53

54
55 CMD - cognitive-motor dissociation
56

57
58 CNN - convolutional neural network
59
60

1
2
3 DA - data augmentation
4

5 DAREPLANE - **DA**ta driven **RE**search **PL**atform for **NE**urotechnology
6

7
8 DBS - deep brain stimulation
9

10 DoC - disorders of consciousness
11

12 ECG - electrocardiography
13

14 ECoG - electrocorticography
15

16
17 EEG - electroencephalography
18

19 EMG - electromyography
20

21
22 EOG - electrooculogram
23

24 ERD - event-related desynchronization
25

26 ERP - Event-related potential
27

28
29 ErrPs - error-related potentials
30

31 ERS - event-related synchronization
32

33 VECoG - endovascular electrocorticography
34

35
36 fNIRS - functional-near infrared spectroscopy
37

38 GR - Generic Recentering
39

40
41 HD - high density
42

43 HFB - high frequency band
44

45 HFD - Higuchi Fractal Dimension
46

47
48 ISPC - Inter-site phase clustering
49

50
51 ITR - information transfer rate
52

53 ICMS - Intracortical microstimulation
54

55
56 MEG - magnetoencephalography
57
58
59
60

1
2
3
4
5
6
7
8
9
10
11
12
13
14
15
16
17
18
19
20
21
22
23
24
25
26
27
28
29
30
31
32
33
34
35
36
37
38
39
40
41
42
43
44
45
46
47
48
49
50
51
52
53
54
55
56
57
58
59
60

MI - motor imagery

NFT - neural field theory

PAR - Personally Assisted Recentering

PD - Parkinson's disease

PICU - Pediatric Intensive Care Unit

RNN - recurrent neural network

sEEG - stereo-electroencephalography

SMR - sensorimotor rhythm

tDCS - transcranial Direct Current Stimulation

uHD - ultra-high density

VR - virtual reality

References

- [1] Metzger S L, Littlejohn K T, Silva A B, Moses D A, Seaton M P, Wang R, Dougherty M E, Liu J R, Wu P, Berger M A, Zhuravleva I, Tu-Chan A, Ganguly K, Anumanchipalli G K and Chang E F 2023 A high-performance neuroprosthesis for speech decoding and avatar control *Nature* **620** 1037–46
- [2] Willett F R, Kunz E M, Fan C, Avansino D T, Wilson G H, Choi E Y, Kamdar F, Glasser M F, Hochberg L R, Druckmann S, Shenoy K V and Henderson J M 2023 A high-performance speech neuroprosthesis *Nature* **620** 1031–6
- [3] Luo S, Rabbani Q and Crone N E 2022 Brain-Computer Interface: Applications to Speech Decoding and Synthesis to Augment Communication *Neurotherapeutics* **19** 263–73
- [4] Berezutskaya J, Freudenburg Z V, Vansteensel M J, Aarnoutse E J, Ramsey N F and van Gerven M A J 2023 Direct speech reconstruction from sensorimotor brain activity with optimized deep learning models *J. Neural Eng.* **20** 056010
- [5] Panachakel J T and Ramakrishnan A G 2021 Decoding Covert Speech From EEG-A Comprehensive Review *Front. Neurosci.* **15**
- [6] Metzger S L, Liu J R, Moses D A, Dougherty M E, Seaton M P, Littlejohn K T, Chartier J, Anumanchipalli G K, Tu-Chan A, Ganguly K and Chang E F 2022 Generalizable spelling using a speech neuroprosthesis in an individual with severe limb and vocal paralysis *Nat. Commun.* **13** 6510
- [7] Verwoert M, Ottenhoff M C, Goulis S, Colon A J, Wagner L, Tousseyn S, van Dijk J P, Kubben P L and Herff C 2022 Dataset of Speech Production in intracranial Electroencephalography *Sci. Data* **9** 434
- [8] Singh A, Hussain A A, Lal S and Guesgen H W 2021 A Comprehensive Review on Critical Issues and Possible Solutions of Motor Imagery Based Electroencephalography Brain-Computer Interface *Sensors* **21** 2173
- [9] Robinson P A, Rennie C J, Rowe D L, O'Connor S C and Gordon E 2005 Multiscale brain modelling *Philos. Trans. R. Soc. B Biol. Sci.* **360** 1043–50
- [10] Tangermann M, Müller K-R, Aertsen A, Birbaumer N, Braun C, Brunner C, Leeb R, Mehring C, Miller K J, Müller-Putz G R, Nolte G, Pfurtscheller G, Preissl H, Schalk G, Schlögl A, Vidaurre C, Waldert S and Blankertz B 2012 Review of the BCI Competition IV *Front. Neurosci.* **6** 55
- [11] Polyakov D, Robinson P A, Muller E J and Shriki O 2024 Recruiting neural field theory for data augmentation in a motor imagery brain-computer interface *Front. Robot. AI* **11** 1362735
- [12] Pfurtscheller G and Neuper C 2001 Motor imagery and direct brain-computer communication *Proc. IEEE* **89** 1123–34
- [13] Little S, Bonaiuto J, Barnes G and Bestmann S 2019 Human motor cortical beta bursts relate to movement planning and response errors *PLoS Biol.* **17** e3000479
- [14] Aristimunha B, Carrara I, Guetschel P, Sedlar S, Rodrigues P, Sosulski J, Narayanan D, Bjareholt E, Barthelemy Q, Schirrmeyer R T, Kobler R, Kalunga E, Darmet L, Gregoire C, Abdul Hussain A, Gatti R,

1
2
3 Goncharenko V, Thielen J, Moreau T, Roy Y, Jayaram V, Barachant A and Chevallier S 2024 Mother of all
4 BCI Benchmarks
5

6 [15] Szul M J, Papadopoulos S, Alavizadeh S, Daligaut S, Schwartz D, Mattout J and Bonaiuto J J 2023
7 Diverse beta burst waveform motifs characterize movement-related cortical dynamics *Prog. Neurobiol.*
8 **228** 102490
9

10 [16] Papadopoulos S, Szul M J, Congedo M, Bonaiuto J J and Mattout J 2024 Beta bursts question the
11 ruling power for brain-computer interfaces *J. Neural Eng.* **21**
12

13 [17] Papadopoulos S, Darmet L, Szul M J, Congedo M, Bonaiuto J J and Mattout J 2024 Surfing beta
14 burst waveforms to improve motor imagery-based BCI 2024.07.18.604064
15

16 [18] Papadopoulos S, Darmet L, Szul M J, Congedo M, Bonaiuto J and Mattout J 2024 Improved
17 motor imagery decoding with spatiotemporal filtering based on beta burst kernels *9th Graz Brain-*
18 *Computer Interface Conference 2024* (Graz, Austria: Verlag der Technischen Universität Graz)
19
20

21 [19] Singh A, Lal S and Guesgen H W 2017 Architectural Review of Co-Adaptive Brain Computer
22 Interface *2017 4th Asia-Pacific World Congress on Computer Science and Engineering (APWC on CSE)*
23 *2017 4th Asia-Pacific World Congress on Computer Science and Engineering (APWC on CSE)* pp 200–7
24

25 [20] Peterson V, Nieto N, Wyser D, Lamercy O, Gassert R, Milone D H and Spies R D 2022 Transfer
26 Learning Based on Optimal Transport for Motor Imagery Brain-Computer Interfaces *IEEE Trans. Biomed.*
27 *Eng.* **69** 807–17
28

29 [21] Lotte F and Guan C 2011 Regularizing Common Spatial Patterns to Improve BCI Designs: Unified
30 Theory and New Algorithms *IEEE Trans. Biomed. Eng.* **58** 355–62
31

32 [22] Pfurtscheller G and Lopes da Silva F H 1999 Event-related EEG/MEG synchronization and
33 desynchronization: basic principles *Clin. Neurophysiol. Off. J. Int. Fed. Clin. Neurophysiol.* **110** 1842–57
34

35 [23] Cattai T, Colonnese S, Corsi M-C, Bassett D S, Scarano G and De Vico Fallani F 2021
36 Phase/Amplitude Synchronization of Brain Signals During Motor Imagery BCI Tasks *IEEE Trans. Neural*
37 *Syst. Rehabil. Eng. Publ. IEEE Eng. Med. Biol. Soc.* **29** 1168–77
38
39

40 [24] Gotts S J, Jo H J, Wallace G L, Saad Z S, Cox R W and Martin A 2013 Two distinct forms of
41 functional lateralization in the human brain *Proc. Natl. Acad. Sci.* **110** E3435–44
42

43 [25] Jayaram V and Barachant A 2018 MOABB: trustworthy algorithm benchmarking for BCIs *J.*
44 *Neural Eng.* **15** 066011
45

46 [26] Millán J d. R, Rupp R, Müller-Putz G R, Murray-Smith R, Giugliemma C, Tangermann M, Vidaurre
47 C, Cincotti F, Kübler A, Leeb R, Neuper C, Müller K-R and Mattia D 2010 Combining Brain-Computer
48 Interfaces and Assistive Technologies: State-of-the-Art and Challenges *Front. Neurosci.* **4** 161
49

50 [27] Biasucci A, Leeb R, Iturrate I, Perdakis S, Al-Khodairy A, Corbet T, Schnider A, Schmidlin T, Zhang
51 H, Bassolino M, Viceic D, Vuadens P, Guggisberg A G and Millán J d R 2018 Brain-actuated functional
52 electrical stimulation elicits lasting arm motor recovery after stroke *Nat. Commun.* **9** 2421
53
54
55
56
57
58
59
60

- 1
2
3 [28] Tonin L, Perdikis S, Kuzu T D, Pardo J, Orset B, Lee K, Aach M, Schildhauer T A, Martínez-Olivera
4 R and Millán J D R 2022 Learning to control a BMI-driven wheelchair for people with severe tetraplegia
5 *iScience* **25** 105418
6
- 7 [29] Perdikis S, Tonin L, Saeedi S, Schneider C and Millán J D R 2018 The Cybathlon BCI race:
8 Successful longitudinal mutual learning with two tetraplegic users *PLoS Biol.* **16** e2003787
9
- 10 [30] Perdikis S and Millan J del R 2020 Brain-Machine Interfaces: A Tale of Two Learners *IEEE Syst.*
11 *Man Cybern. Mag.* **6** 12–9
12
- 13 [31] Kumar S, Alawieh H, Racz F S, Fakhreddine R and Millán J D R 2024 Transfer learning promotes
14 acquisition of individual BCI skills *PNAS Nexus* **3** pgae076
15
- 16 [32] Zanini P, Congedo M, Jutten C, Said S and Berthoumieu Y 2018 Transfer Learning: A Riemannian
17 Geometry Framework With Applications to Brain–Computer Interfaces *IEEE Trans. Biomed. Eng.* **65**
18 1107–16
19
- 20 [33] Kumar S, Yger F and Lotte F 2019 Towards Adaptive Classification using Riemannian Geometry
21 approaches in Brain–Computer Interfaces *2019 7th International Winter Conference on Brain–Computer*
22 *Interface (BCI) 2019 7th International Winter Conference on Brain-Computer Interface (BCI)* pp 1–6
23
- 24 [34] Leeb R, Perdikis S, Tonin L, Biasiucci A, Tavella M, Creatura M, Molina A, Al-Khodairy A, Carlson
25 T and Millán J D R 2013 Transferring brain-computer interfaces beyond the laboratory: successful
26 application control for motor-disabled users *Artif. Intell. Med.* **59** 121–32
27
- 28 [35] Anon Brain-Computer Interface Race
29
- 30 [36] Lotte F and Jeunet C 2018 Defining and quantifying users' mental imagery-based BCI skills: a
31 first step *J. Neural Eng.* **15** 046030
32
- 33 [37] Lawhern V J, Solon A J, Waytowich N R, Gordon S M, Hung C P and Lance B J 2016 EEGNet: A
34 Compact Convolutional Network for EEG-based Brain-Computer Interfaces *arXiv.org*
35
- 36 [38] Kobler R J, Hirayama J, Zhao Q and Kawanabe M 2022 SPD domain-specific batch normalization
37 to crack interpretable unsupervised domain adaptation in EEG *arXiv.org*
38
- 39 [39] Rossiter H E, Boudrias M-H and Ward N S 2014 Do movement-related beta oscillations change
40 after stroke? *J. Neurophysiol.* **112** 2053–8
41
- 42 [40] Orlandi S, House S C, Karlsson P, Saab R and Chau T 2021 Brain-Computer Interfaces for
43 Children With Complex Communication Needs and Limited Mobility: A Systematic Review *Front. Hum.*
44 *Neurosci.* **15** 643294
45
- 46 [41] Fadhli M, Brick B, Setyosari P, Ulfa S and Kuswandi D 2020 A Meta-Analysis of Selected Studies
47 on the Effectiveness of Gamification Method for Children *Int. J. Instr.* **13** 845–54
48
- 49 [42] Mikołajewska E and Mikołajewski D 2014 The prospects of brain — computer interface
50 applications in children *Open Med.* **9** 74–9
51
52
53
54
55
56
57
58
59
60

- 1
2
3 [43] Keough J R, Irvine B, Kelly D, Wrightson J, Comaduran Marquez D, Kinney-Lang E and Kirton A
4 2024 Fatigue in children using motor imagery and P300 brain-computer interfaces *J. Neuroengineering*
5 *Rehabil.* **21** 61
6
7 [44] Edlow B L, Claassen J, Schiff N D and Greer D M 2021 Recovery from disorders of consciousness:
8 mechanisms, prognosis and emerging therapies *Nat. Rev. Neurol.* **17** 135–56
9
10 [45] Jadavji Z, Zewdie E, Kelly D, Kinney-Lang E, Robu I and Kirton A Establishing a Clinical Brain-
11 Computer Interface Program for Children With Severe Neurological Disabilities *Cureus* **14** e26215
12
13 [46] Natalie Mrachacz-Kersting, Jennifer Collinger, Donatella Mattia, Davide Valeriani, Mariska
14 Vansteensel, and Gernot Müller-Putz 10th International BCI Meeting 2023 Abstract Book; Balancing
15 Innovation and Translation; June 6 - 9, 2023, Sonian Forest, Brussels, Belgium (Verlag der Technischen
16 Universität Graz)
17
18 [47] Oehrnc R, Cernera S, Hammer L H, Shcherbakova M, Yao J, Hahn A, Wang S, Ostrem J L, Little S
19 and Starr P A 2023 Personalized chronic adaptive deep brain stimulation outperforms conventional
20 stimulation in Parkinson’s disease 2023.08.03.23293450
21
22 [48] Opri E, Cernera S, Molina R, Eisinger R S, Cagle J N, Almeida L, Denison T, Okun M S, Foote K D
23 and Gunduz A 2020 Chronic embedded cortico-thalamic closed-loop deep brain stimulation for the
24 treatment of essential tremor *Sci. Transl. Med.* **12** eaay7680
25
26 [49] Wang W, Collinger J L, Degenhart A D, Tyler-Kabara E C, Schwartz A B, Moran D W, Weber D J,
27 Wodlinger B, Vinjamuri R K, Ashmore R C, Kelly J W and Boninger M L 2013 An electrocorticographic
28 brain interface in an individual with tetraplegia *PloS One* **8** e55344
29
30 [50] Dold M, Pereira J, Sajonz B, Coenen V A, Janssen M L F and Tangermann M 2024 A modular
31 open-source software platform for BCI research with application in closed-loop deep brain stimulation
32
33 [51] Herz D M, Little S, Pedrosa D J, Tinkhauser G, Cheeran B, Foltynie T, Bogacz R and Brown P 2018
34 Mechanisms Underlying Decision-Making as Revealed by Deep-Brain Stimulation in Patients with
35 Parkinson’s Disease *Curr. Biol. CB* **28** 1169-1178.e6
36
37 [52] Gao Q, Schmidt S L, Chowdhury A, Feng G, Peters J J, Genty K, Grill W M, Turner D A and Pajic M
38 2023 Offline Learning of Closed-Loop Deep Brain Stimulation Controllers for Parkinson Disease
39 Treatment *Proceedings of the ACM/IEEE 14th International Conference on Cyber-Physical Systems (with*
40 *CPS-IoT Week 2023) ICCPS ’23* (New York, NY, USA: Association for Computing Machinery) pp 44–55
41
42 [53] Castaño-Candamil S, Piroth T, Reinacher P, Sajonz B, Coenen V A and Tangermann M 2020
43 Identifying controllable cortical neural markers with machine learning for adaptive deep brain
44 stimulation in Parkinson’s disease *NeuroImage Clin.* **28** 102376
45
46 [54] Swann N C, de Hemptinne C, Thompson M C, Miocinovic S, Miller A M, Gilron R, Ostrem J L,
47 Chizeck H J and Starr P A 2018 Adaptive deep brain stimulation for Parkinson’s disease using motor
48 cortex sensing *J. Neural Eng.* **15** 046006
49
50 [55] Bocci T, Prenassi M, Arlotti M, Cogiamanian F M, Borellini L, Moro E, Lozano A M, Volkmann J,
51 Barbieri S, Priori A and Marceglia S 2021 Eight-hours conventional versus adaptive deep brain
52 stimulation of the subthalamic nucleus in Parkinson’s disease *NPJ Park. Dis.* **7** 88
53
54
55
56
57
58
59
60

- 1
2
3 [56] Oehrns C R, Cernera S, Hammer L H, Shcherbakova M, Yao J, Hahn A, Wang S, Ostrem J L, Little S
4 and Starr P A 2024 Chronic adaptive deep brain stimulation versus conventional stimulation in
5 Parkinson's disease: a blinded randomized feasibility trial *Nat. Med.* 1–12
6
7 [57] Kothe C 2024 sccn/labstreaminglayer
8
9 [58] Castano-Candamil S, Piroth T, Reinacher P, Sajonz B, Coenen V A and Tangermann M 2019 An
10 Easy-to-Use and Fast Assessment of Patient-Specific DBS-Induced Changes in Hand Motor Control in
11 Parkinson's Disease *IEEE Trans. Neural Syst. Rehabil. Eng. Publ. IEEE Eng. Med. Biol. Soc.* **27** 2155–63
12
13 [59] Hossain K M, Islam M A, Hossain S, Nijholt A and Ahad M A R 2023 Status of deep learning for
14 EEG-based brain–computer interface applications *Front. Comput. Neurosci.* **16**
15
16 [60] Han Y, Valentini E and Halder S 2022 Classification of Tonic Pain Experience based on Phase
17 Connectivity in the Alpha Frequency Band of the Electroencephalogram using Convolutional Neural
18 Networks 2022 44th Annual International Conference of the IEEE Engineering in Medicine & Biology
19 Society (EMBC) 2022 44th Annual International Conference of the IEEE Engineering in Medicine &
20 Biology Society (EMBC) pp 3542–5
21
22 [61] Horing B, Sprenger C and Büchel C 2019 The parietal operculum preferentially encodes heat
23 pain and not salience *PLOS Biol.* **17** e3000205
24
25 [62] Mari T, Henderson J, Maden M, Nevitt S, Duarte R and Fallon N 2022 Systematic Review of the
26 Effectiveness of Machine Learning Algorithms for Classifying Pain Intensity, Phenotype or Treatment
27 Outcomes Using Electroencephalogram Data *J. Pain* **23** 349–69
28
29 [63] Furman A J, Meeker T J, Rietschel J C, Yoo S, Muthulingam J, Prokhorenko M, Keaser M L,
30 Goodman R N, Mazaheri A and Seminowicz D A 2018 Cerebral peak alpha frequency predicts individual
31 differences in pain sensitivity *NeuroImage* **167** 203–10
32
33 [64] Salomons T V, Johnstone T, Backonja M-M, Shackman A J and Davidson R J 2007 Individual
34 differences in the effects of perceived controllability on pain perception: critical role of the prefrontal
35 cortex *J. Cogn. Neurosci.* **19** 993–1003
36
37 [65] Han Y, Valentini E and Halder S 2023 Validation of Cross-Individual Pain Assessment with
38 Individual Recognition Model from Electroencephalogram 2023 45th Annual International Conference of
39 the IEEE Engineering in Medicine & Biology Society (EMBC) 2023 45th Annual International Conference
40 of the IEEE Engineering in Medicine & Biology Society (EMBC) pp 1–4
41
42 [66] Glaser J I, Benjamin A S, Farhoodi R and Kording K P 2019 The roles of supervised machine
43 learning in systems neuroscience *Prog. Neurobiol.* **175** 126–37
44
45 [67] Tseng P-H, Urpi N A, Lebedev M and Nicolelis M 2019 Decoding Movements from Cortical
46 Ensemble Activity Using a Long Short-Term Memory Recurrent Network *Neural Comput.* **31** 1085–113
47
48 [68] Livezey J A, Bouchard K E and Chang E F 2019 Deep learning as a tool for neural data analysis:
49 Speech classification and cross-frequency coupling in human sensorimotor cortex *PLoS Comput. Biol.* **15**
50 e1007091
51
52
53
54
55
56
57
58
59
60

- 1
2
3 [69] Neumann W-J, Gilron R, Little S and Tinkhauser G 2023 Adaptive Deep Brain Stimulation: From
4 Experimental Evidence Toward Practical Implementation *Mov. Disord. Off. J. Mov. Disord. Soc.* **38** 937–
5 48
6
7 [70] Merk T, Peterson V, Köhler R, Haufe S, Richardson R M and Neumann W-J 2022 Machine
8 learning based brain signal decoding for intelligent adaptive deep brain stimulation *Exp. Neurol.* **351**
9 113993
10
11 [71] Colucci A, Vermehren M, Cavallo A, Angerhöfer C, Peekhaus N, Zollo L, Kim W-S, Paik N-J and
12 Soekadar S R 2022 Brain-Computer Interface-Controlled Exoskeletons in Clinical Neurorehabilitation:
13 Ready or Not? *Neurorehabil. Neural Repair* **36** 747–56
14
15 [72] Al-Quraishi M S, Elamvazuthi I, Daud S A, Parasuraman S and Borboni A 2018 EEG-Based Control
16 for Upper and Lower Limb Exoskeletons and Prostheses: A Systematic Review *Sensors* **18** 3342
17
18 [73] Buccelli S, Tessari F, Fanin F, De Guglielmo L, Capitta G, Piezzo C, Bruschi A, Van Son F, Scarpetta
19 S, Succi A, Rossi P, Maludrotto S, Barresi G, Creatini I, Taglione E, Laffranchi M and De Michieli L 2022 A
20 Gravity-Compensated Upper-Limb Exoskeleton for Functional Rehabilitation of the Shoulder Complex
21 *Appl. Sci.* **12** 3364
22
23 [74] Garro F, Fenoglio E, Forsiuk I, Canepa M, Mozzon M, De Michieli L, Buccelli S, Chiappalone M
24 and Semprini M 2023 NeBULA: A Standardized Protocol for the Benchmarking of Robotic-based Upper
25 Limb Neurorehabilitation 2023 45th Annual International Conference of the IEEE Engineering in Medicine
26 & Biology Society (EMBC) 2023 45th Annual International Conference of the IEEE Engineering in
27 Medicine & Biology Society (EMBC) pp 1–4
28
29 [75] Choi S W, Chi S E, Chung S Y, Kim J W, Ahn C Y and Kim H T 2011 Is alpha wave neurofeedback
30 effective with randomized clinical trials in depression? A pilot study *Neuropsychobiology* **63** 43–51
31
32 [76] Trambaiolli L R, Kohl S H, Linden D E J and Mehler D M A 2021 Neurofeedback training in major
33 depressive disorder: A systematic review of clinical efficacy, study quality and reporting practices
34 *Neurosci. Biobehav. Rev.* **125** 33–56
35
36 [77] Vujic A, Nisal S and Maes P 2023 Joie: a Joy-based Brain-Computer Interface (BCI) *Proceedings*
37 *of the 36th Annual ACM Symposium on User Interface Software and Technology* UIST '23 (New York, NY,
38 USA: Association for Computing Machinery) pp 1–14
39
40 [78] Vujic A, Martin A, Nisal S, Mohammed M and Maes P 2023 Demonstration of Joie: A Joy-based
41 Brain-Computer Interface (BCI) with Wearable Skin Conformal Polymer Electrodes *Adjunct Proceedings*
42 *of the 36th Annual ACM Symposium on User Interface Software and Technology* UIST '23 Adjunct (New
43 York, NY, USA: Association for Computing Machinery) pp 1–3
44
45 [79] Oxley T J, Yoo P E, Rind G S, Ronayne S M, Lee C M S, Bird C, Hampshire V, Sharma R P, Morokoff
46 A, Williams D L, Maclsaac C, Howard M E, Irving L, Vrljic I, Williams C, John S E, Weissenborn F, Dzenko
47 M, Balabanski A H, Friedenberg D, Burkitt A N, Wong Y T, Drummond K J, Desmond P, Weber D, Denison
48 T, Hochberg L R, Mathers S, O'Brien T J, May C N, Mocco J, Grayden D B, Campbell B C V, Mitchell P and
49 Opie N L 2021 Motor neuroprosthesis implanted with neurointerventional surgery improves capacity for
50 activities of daily living tasks in severe paralysis: first in-human experience *J. NeuroInterventional Surg.*
51 **13** 102–8
52
53
54
55
56
57
58
59
60

- 1
2
3 [80] Jasper H H 1958 The Ten-Twenty Electrode System of the International Federation
4 *Electroencephalography and Clinical Neurophysiology* **10** 371–5
5
- 6 [81] Chatrian G E, Lettich E and Nelson P L 1985 Ten Percent Electrode System for Topographic
7 Studies of Spontaneous and Evoked EEG Activities *Am. J. EEG Technol.* **25** 83–92
8
- 9 [82] Oostenveld R and Praamstra P 2001 The five percent electrode system for high-resolution EEG
10 and ERP measurements *Clin. Neurophysiol. Off. J. Int. Fed. Clin. Neurophysiol.* **112** 713–9
11
- 12 [83] Lee H S, Schreiner L, Jo S-H, Sieghartsleitner S, Jordan M, Pretl H, Guger C and Park H-S 2022
13 Individual finger movement decoding using a novel ultra-high-density electroencephalography-based
14 brain-computer interface system *Front. Neurosci.* **16** 1009878
15
- 16 [84] Bera S, Roy R, Sikdar D and Mahadevappa M 2019 An Ensemble Learning Based Classification of
17 Individual Finger Movement from EEG
18
- 19 [85] Liao K, Xiao R, Gonzalez J and Ding L 2014 Decoding Individual Finger Movements from One
20 Hand Using Human EEG Signals *PLoS ONE* **9** e85192
21
- 22 [86] Schreiner L, Sieghartsleitner S, Mayr K, Pretl H and Guger C 2023 Hand gesture decoding using
23 ultra-high-density EEG 2023 11th International IEEE/EMBS Conference on Neural Engineering (NER) 2023
24 11th International IEEE/EMBS Conference on Neural Engineering (NER) pp 01–4
25
- 26 [87] Branco M P, Geukes S H, Aarnoutse E J, Ramsey N F and Vansteensel M J 2023 Nine decades of
27 electrocorticography: A comparison between epidural and subdural recordings *Eur. J. Neurosci.* **57**
28 1260–88
29
- 30 [88] Flinker A, Chang E F, Barbaro N M, Berger M S and Knight R T 2011 Sub-centimeter language
31 organization in the human temporal lobe *Brain Lang.* **117** 103–9
32
- 33 [89] Menon V, Freeman W J, Cutillo B A, Desmond J E, Ward M F, Bressler S L, Laxer K D, Barbaro N
34 and Gevins A S 1996 Spatio-temporal correlations in human gamma band electrocorticograms
35 *Electroencephalogr. Clin. Neurophysiol.* **98** 89–102
36
- 37 [90] Geukes S H, Branco M P, Aarnoutse E J, Bekius A, Berezutskaya J and Ramsey N F 2024 Effect of
38 Electrode Distance and Size on Electrocorticographic Recordings in Human Sensorimotor Cortex
39 *Neuroinformatics* **22** 707–17
40
- 41 [91] Flesher S N, Collinger J L, Foldes S T, Weiss J M, Downey J E, Tyler-Kabara E C, Bensmaia S J,
42 Schwartz A B, Boninger M L and Gaunt R A 2016 Intracortical microstimulation of human somatosensory
43 cortex *Sci. Transl. Med.* **8** 361ra141-361ra141
44
- 45 [92] Flesher S N, Downey J E, Weiss J M, Hughes C L, Herrera A J, Tyler-Kabara E C, Boninger M L,
46 Collinger J L and Gaunt R A 2021 A brain-computer interface that evokes tactile sensations improves
47 robotic arm control *Science* **372** 831–6
48
- 49 [93] Chavarriaga R, Sobolewski A and Millán J del R 2014 Errare machinale est: the use of error-
50 related potentials in brain-machine interfaces *Front. Neurosci.* **8**
51
52
53
54
55
56
57
58
59
60

- 1
2
3 [94] Wimmer M, Weidinger N, Veas E and Muller-Putz G R 2023 Neural and Pupillometric Correlates
4 of Error Perception in an Immersive VR Flight Simulation *Annu. Int. Conf. IEEE Eng. Med. Biol. Soc. IEEE*
5 *Eng. Med. Biol. Soc. Annu. Int. Conf.* **2023** 1–4
6
7 [95] Wimmer M, Weidinger N, Veas E and Müller-Putz G R 2024 Multimodal decoding of error
8 processing in a virtual reality flight simulation *Sci. Rep.* **14** 9221
9
10 [96] Wimmer M, Weidinger N, ElSayed N, Müller-Putz G R and Veas E 2023 EEG-Based Error
11 Detection Can Challenge Human Reaction Time in a VR Navigation Task 2023 IEEE International
12 Symposium on Mixed and Augmented Reality (ISMAR) (IEEE Computer Society) pp 970–9
13
14 [97] Keeser D, Meindl T, Bor J, Palm U, Pogarell O, Mulert C, Brunelin J, Möller H-J, Reiser M and
15 Padberg F 2011 Prefrontal Transcranial Direct Current Stimulation Changes Connectivity of Resting-State
16 Networks during fMRI *J. Neurosci.* **31** 15284–93
17
18 [98] Beeli G, Koeneke S, Gasser K and Jancke L 2008 Brain stimulation modulates driving behavior
19 *Behav. Brain Funct.* **4** 34
20
21 [99] Schreuder M, Höhne J, Blankertz B, Haufe S, Dickhaus T and Tangermann M 2013 Optimizing
22 event-related potential based brain–computer interfaces: a systematic evaluation of dynamic stopping
23 methods *J. Neural Eng.* **10** 036025
24
25 [100] Trees H L V 2004 *Detection, Estimation, and Modulation Theory, Part I: Detection, Estimation,*
26 *and Linear Modulation Theory* (John Wiley & Sons)
27
28 [101] Thielen J, van den Broek P, Farquhar J and Desain P 2015 Broad-Band Visually Evoked
29 Potentials: Re(con)volution in Brain-Computer Interfacing *PloS One* **10** e0133797
30
31
32
33
34
35
36
37
38
39
40
41
42
43
44
45
46
47
48
49
50
51
52
53
54
55
56
57
58
59
60